Activities at AIUB

Astronomisches Institut

Satellite Geodesy Research Group

D. Arnold, E. Calero, R. Dach, N. Darbeheshti, W. Desprats, P. Fridez, C. Gattano, L. Geisser, T. Grombein, A. Jäggi, M. Lasser, M. Kalarus, C. Kobel, X. Mao, U. Meyer, L. Prange, S. Schaer, L. Schreiter, P. Stebler, A. Villiger

Satellite Geodesy Research Group

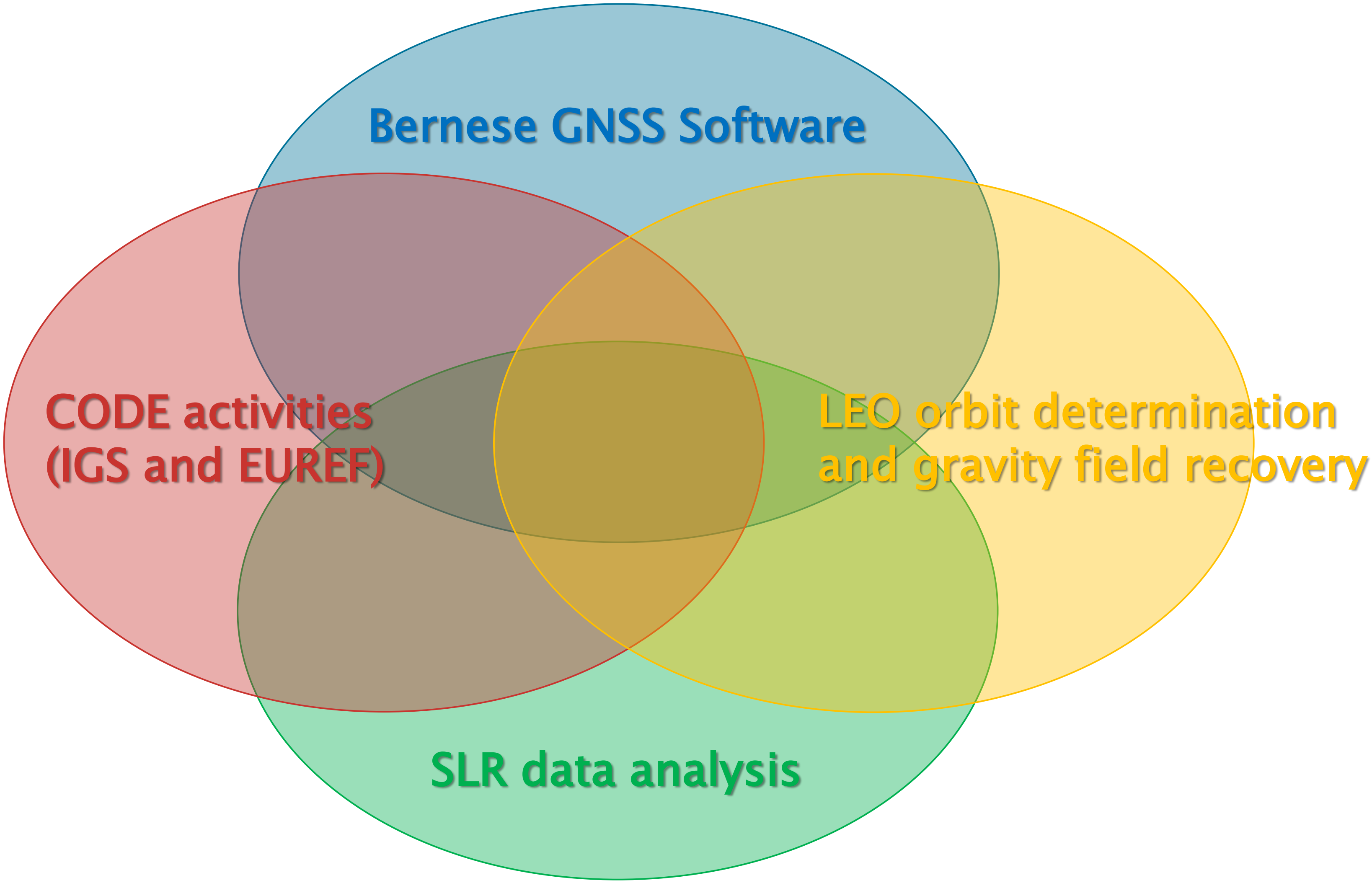

Satellite Geodesy Research Group

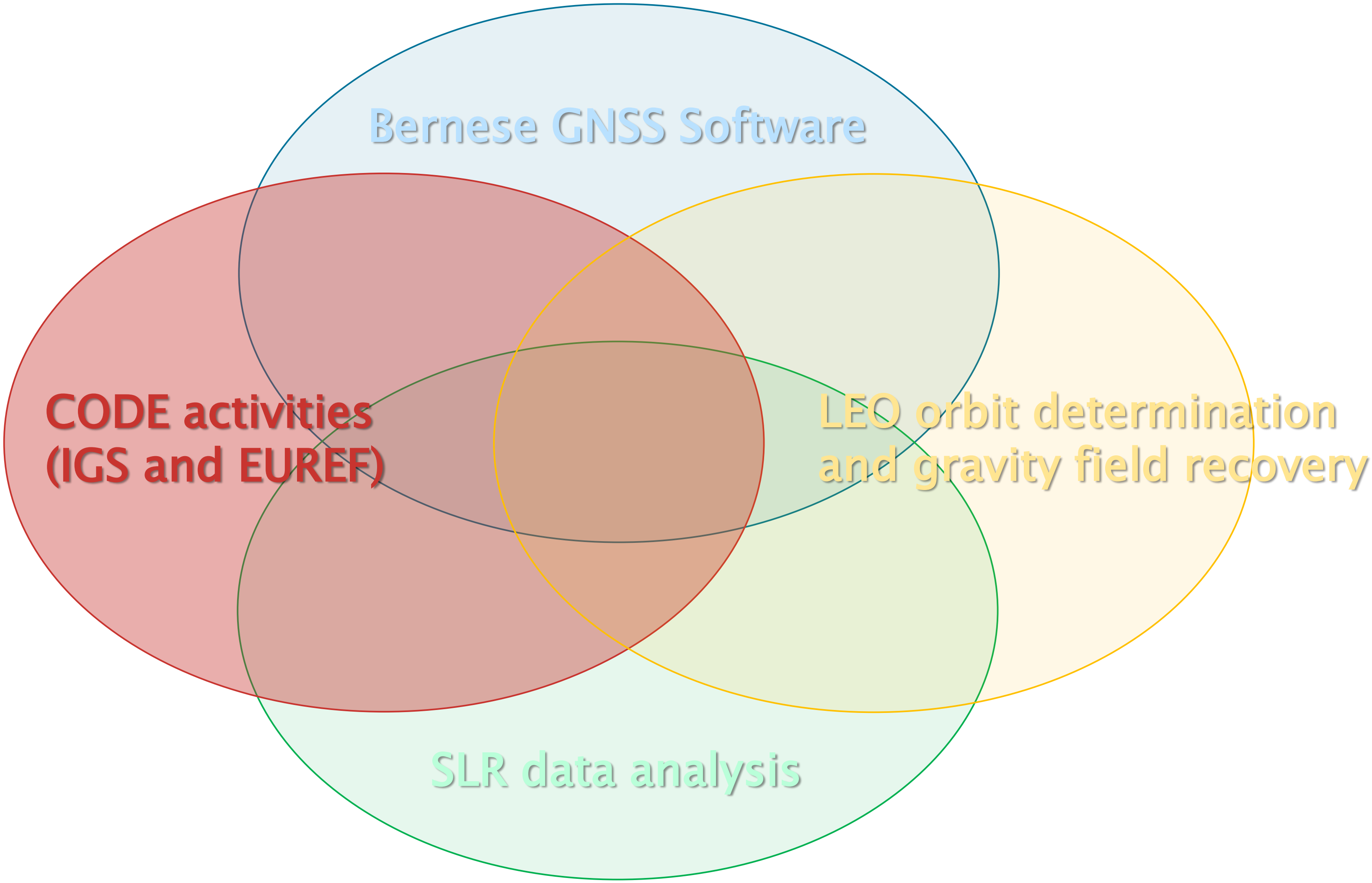

Addendum to report 2020: Reprocessing effort for ITRF2020

CODEs repro results are now available:

- Products are publicly available at
  ftp://ftp.aiub.unibe.ch/REPRO_2020/
  since March 2021.
- Reference:
  Selmke, I., R. Dach, D. Arnold, L. Prange, S. Schaer, D. Sidorov, P. Stebler, A. Villiger, A. Jäggi, U. Hugentobler (2020).CODE repro3 product series for the IGS. Published by Astronomical Institute, University of Bern.
  DOI: 10.7892/boris.135946.
- Paper on modelling improvements:
  Dach, R., I. Selmke, A. Villiger, D. Arnold, L. Prange, S. Schaer, D. Sidorov, P. Stebler, A. Jäggi, U. Hugentobler; 2021: Review of recent GNSS modelling improvements based on CODEs Repro3 contribution.
  Advances in Space Research, 68(3), 1263–1280,
  DOI: 10.1016/j.asr.2021.04.046.

CODE for MGEX: BDS-3

Lars Prange

Why to consider BeiDou 3?

- Operational BDS3 space segment seems fully deployed since 2020
- Signals supported by RINEX3.04 data format and by receivers
- System meanwhile sufficiently supported by IGS tracking network
- System supported by other MGEX ACs (WHU, SHAO, GFZ)
- Interest by MGEX users

⇒ Adaptation of latest BSW (e.g., frequencies, SVN ranges, maxes, …)
⇒ 27 additional satellites (90 => 117); BDS2+3: 37 satellites in total
⇒ BDS frequency selection changed (C2I/X + C7I/X => C2I/X + C6I/X)
⇒ Meta data imported from igs_metadata.snx
⇒ MGEX test solution in early 2021 (2 months of orbits, 1 month of clocks) computed and validated
⇒ No real show-stoppers detected - although BeiDou is the most complex GNSS

Orbit validation

SLR	Median [cm]	IQR [cm]
GLONASS	1.1	4.8
Galileo	-0.6	2.5
BDS	1.3 (1.8)	5.2 (7.5)
QZSS	2.4	9.9
3D orbit misclosures		
GPS	0.8	0.5
GLONASS	1.3	1.2
Galileo	1.0	0.6
BDS	2.8 (2.1)	1.8 (1.6)
QZSS	4.7	3.7
RMS of 3-day long arc orbit fit		
GPS	0.8	0.5
GLONASS	1.8	1.1
Galileo	2.1	1.0
BDS	2.2 (1.7)	1.3 (1.2)
QZSS	3.8	2.6

⇒ Solutions including BDS3 (in brackets) are better w.r.t. long arc fit and orbit misclosures

⇒ SLR statistics is degraded (note that only a subset of the BDS satellites is tracked by SLR)

Clock validation

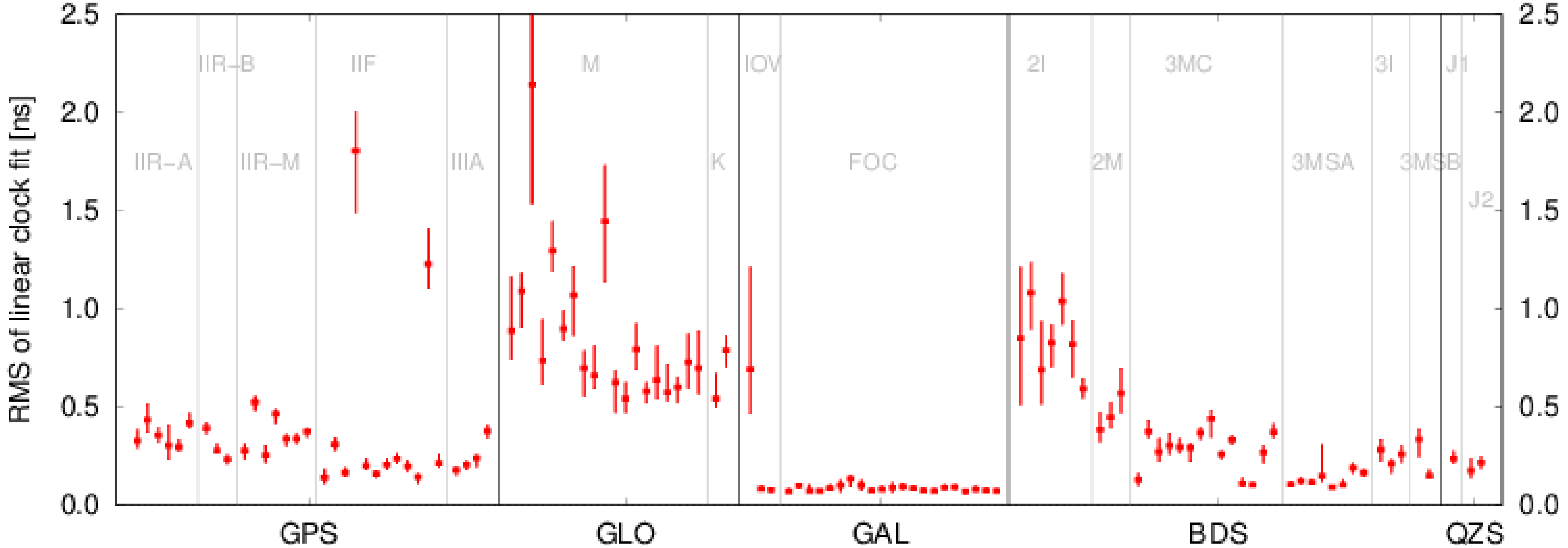

CLK fit	Median [ns]	IQR [ns]
GPS	0.287	0.188
GPS IIIA	0.222	0.100
GLONASS	0.774	0.436
Galileo	0.083	0.035
BDS	0.289	0.290
BDS 3M SECM A	0.125	0.064
QZSS	0.221	0.080

⇒ Linear clock fit indicates good quality of BDS3 satellite clocks - especially for SECM MEOs equipped with PHMs

CODE for IGS

CODE AC team

Selected improvements in the daily processing

- Modelling advances in CODE processing:
  - ORBEX files reporting satellite attitude is published for final and MGEX solution.
  - Switch from VMF1/GMF1 to VMF3/GMF3 troposphere modelling.
  - Consider not-nominal orientation of GNSS antennas (will become relevant for ITRF2020).
  - Rapid and ultra-rapid orbit files with 5 instead of 15 minutes sampling (because of Galileo).

Selected improvements in the daily processing

- Bernese technical advances:
  - Serval file types (BRD, TAB) and 10 programs became dispensable and have been removed from the system.
  - New more flexible BPE file format designed and introduced.
  - BPE and GUI go to Qt5 (until now Qt3-based).

  - Fortran 2003 applied where useful, for example...

Boxwing model error propagation into GNSS global solutions

Maciej Kalarus

Error propagation: box–wing into GNSS–sol.

Simulation setup – box-wing mismodelling

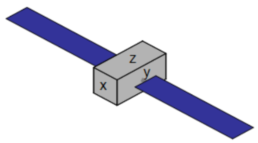

REFERENCE satellite box-wing model (used to generate **REFERENCE** solution)

modified box-wing models

case 1

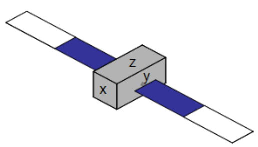

area of solar panels reduced by 50%

case 2

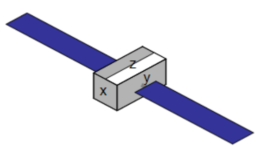

area of plane ***-z*** and ***+z*** (facing the Earth's surface) reduced by 50%

case 3

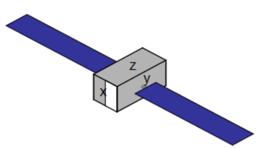

area of plane ***-x*** and ***+x*** reduced by 50%

Note:
Substantial box-wing mismodelling was applied to emphasise the effect in the solution. This can be scaled down to more reasonable values.

Error propagation: box-wing into GNSS-sol.

Results – signatures of the NGP mismodelling

L: epoch-wise clocks **M:** clock modelling applied

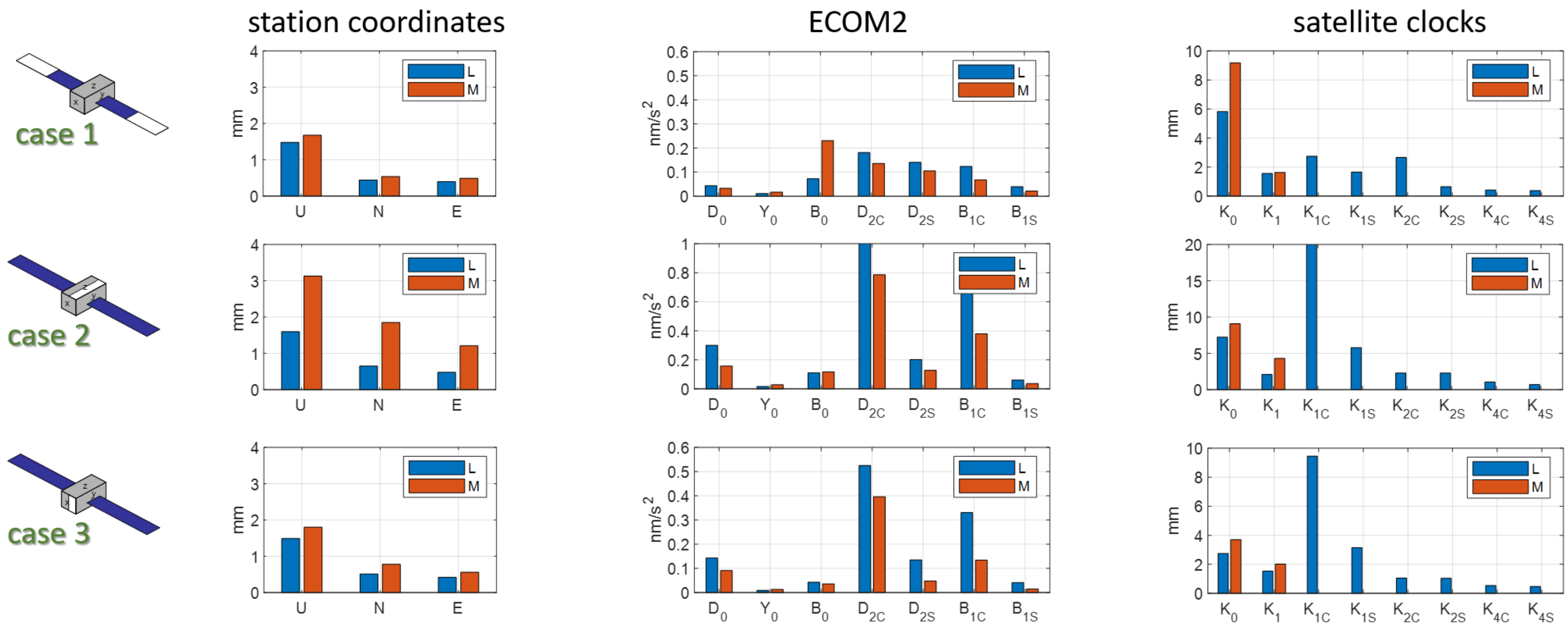

- signatures (values averaged over one year) are based on the solution with all ambiguities resolved
- signatures may give a hint regarding the possible origin of the mismodelled NGP
- another signatures are needed to clearly distinguish between case 2 and 3

Ambiguity resolution in a zero-difference solution

Emilio Calero

Astronomical Institute University of Bern AIUB

Procedure for clock estimation with ambiguity resolution

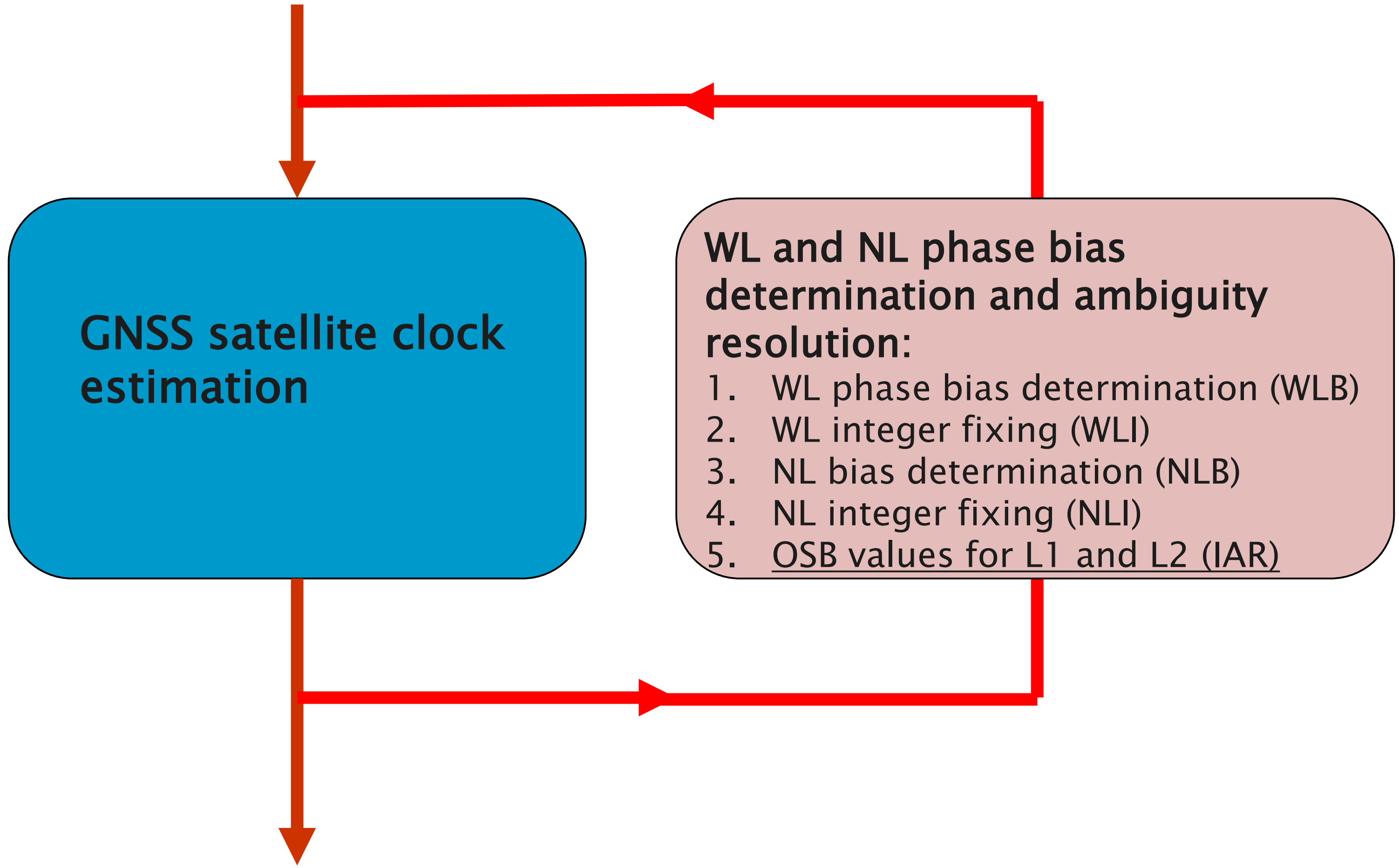

Activated for rapid, final, and MGEX clocks in July 2018

Zero-difference ambiguity resolution at CODE

- Currently the zero-difference ambiguity resolution is based on the known geometry from the double-difference solution.
- PhD from Emilio Calero is advancing this algorithm for the scenario of simultaneous estimation of geometry parameters and phase biases.

Zero-difference ambiguity resolution at CODE

- **Equivalent performance of the new prototype algorithm (ZDM) to the current approach at CODE (example comparison with MGEX for 11 days)**

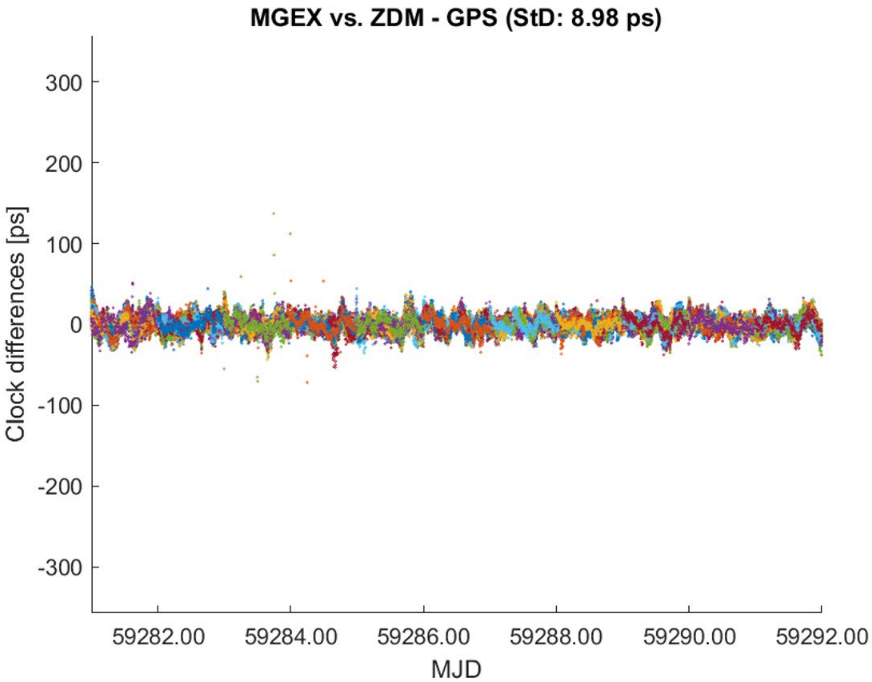

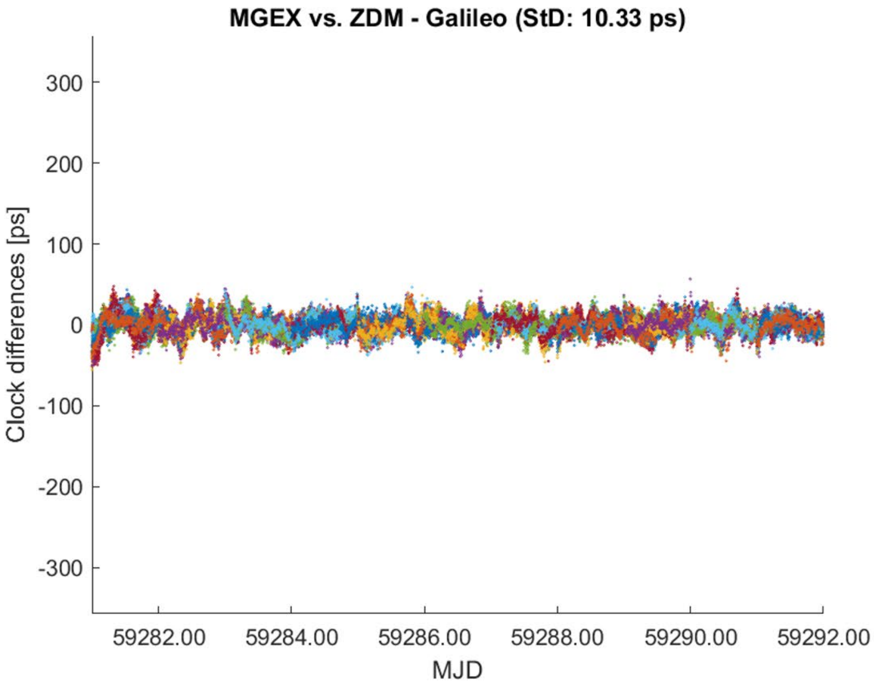

Bernese GNSS Software goes VLBI

César Gattano

Bernese GNSS Software goes VLBI

- A technical challenge is that the measurements may refer not only to satellites but also to quasars with a different characteristics.
- The solution is provided with derived types in Fortran 2003:

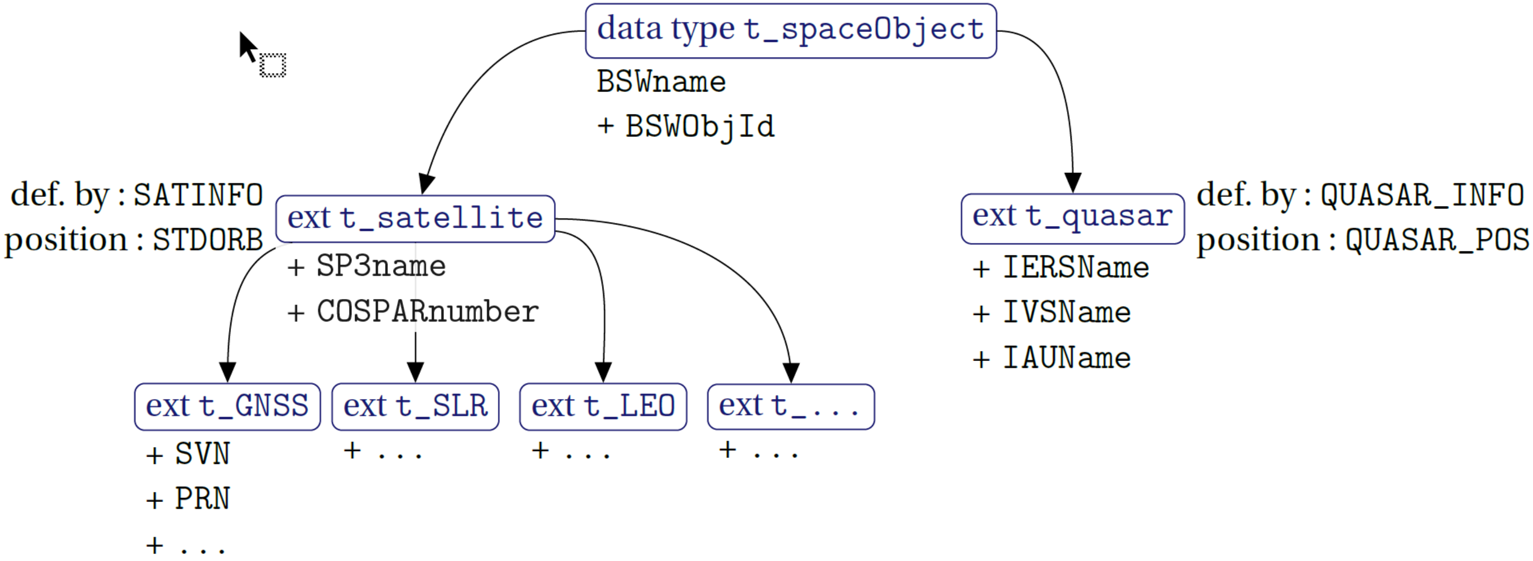

t_spaceObject class

Class hierarchy :

```
TYPE t_spaceObj
   ! Attributes
   ! ----------
   [...]
CONTAINS
   ! Methods
   ! -------
   [...]
END TYPE t_spaceObj
```

```
TYPE, EXTENDS(t_spaceObj) :: &
      t_satellite
   [...]
END TYPE t_satellite
```

```
TYPE, EXTENDS(t_spaceObj) :: &
      t_quasar
   [...]
END TYPE t_quasar
```

```
TYPE, EXTENDS(t_satellite) :: t_GNSSSatellite
   [...]
```

```
TYPE, EXTENDS(t_satellite) :: t_SLRCannonBall
   [...]
```

```
TYPE, EXTENDS(t_satellite) :: t_LEOSatellite
   [...]
END TYPE t_LEOSatellite
```

Satellite Geodesy Research Group

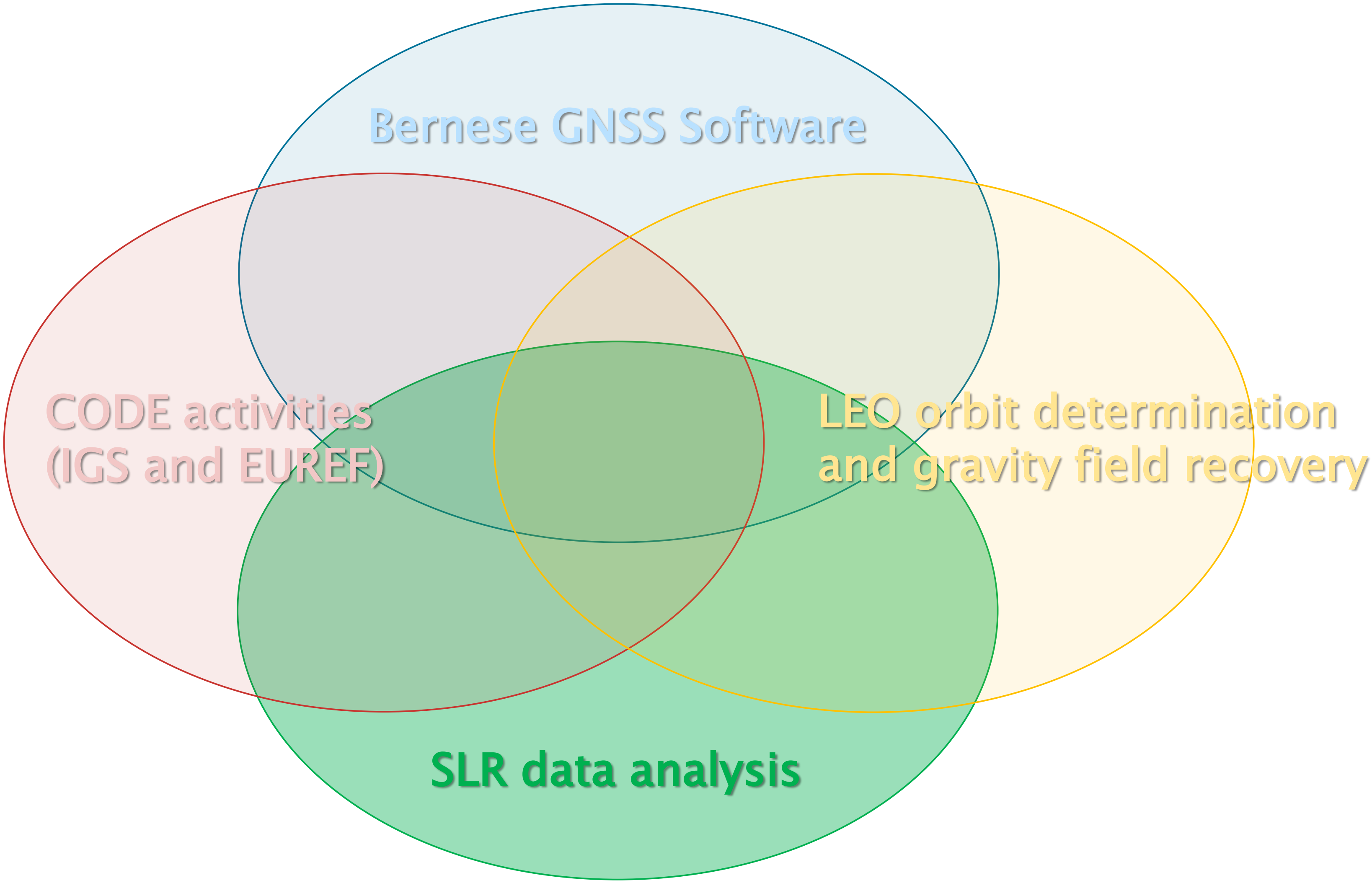

Reprocessing effort for ITRF2020

Ulrich Meyer

ITRF2020-Repro

AIUB collaborates with BKG (Germany) on the ILRS reprocessing campaign of weekly LAGEOS/ETALON combined solutions for ITRF2020.

LAGEOS/ETALON observation statistics and RMS of weekly network solutions

<table>
<tr><th></th><th>LAGEOS (L7A)</th><th>ETALON (L7B)</th><th>Combination (C7_)</th></tr>
<tr><td>observations</td><td>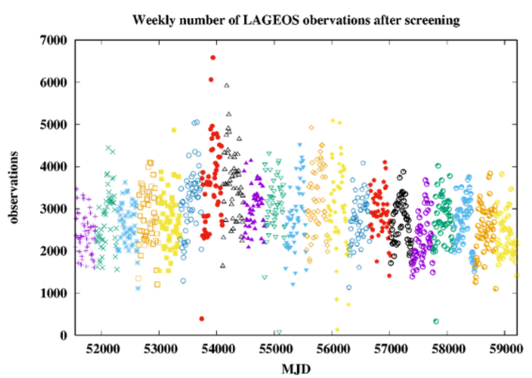
</td><td>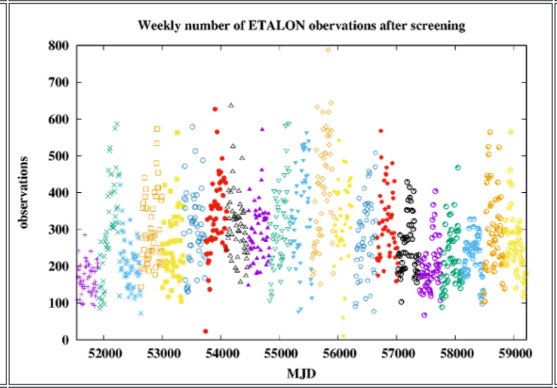
</td><td></td></tr>
<tr><td>RMS</td><td>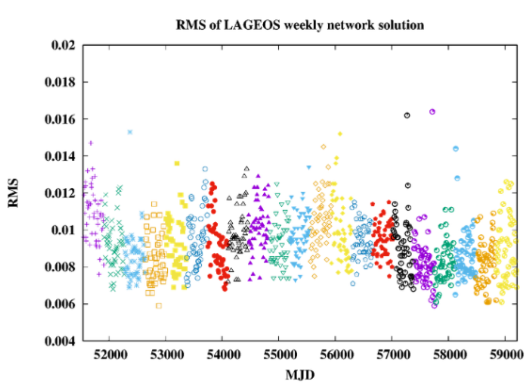
</td><td></td><td>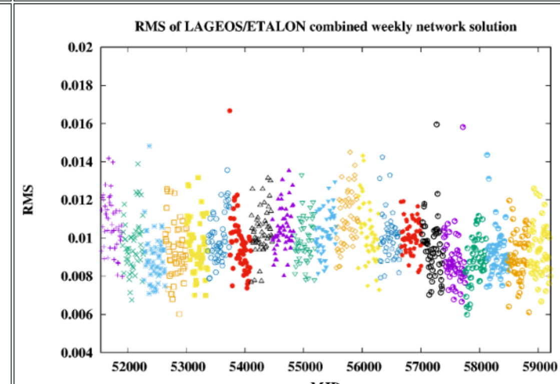
</td></tr>
</table>

ITRF2020-Repro

The weekly network solutions contain station coordinates, range biases for pre-defined stations and time-periods, and Earth rotation parameters.

Station coordinates (example stations)

Graz 7839	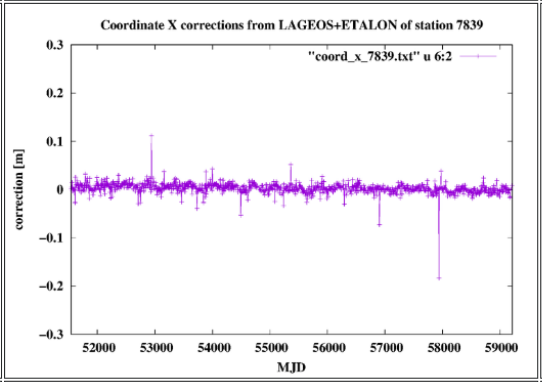	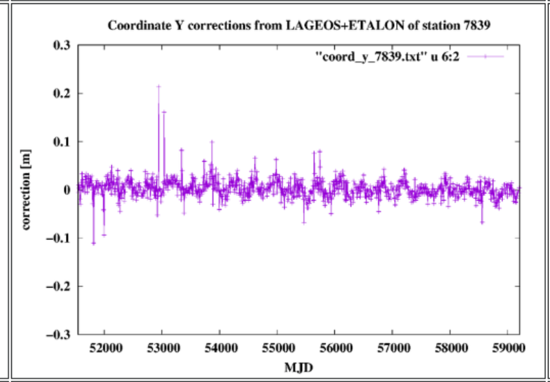	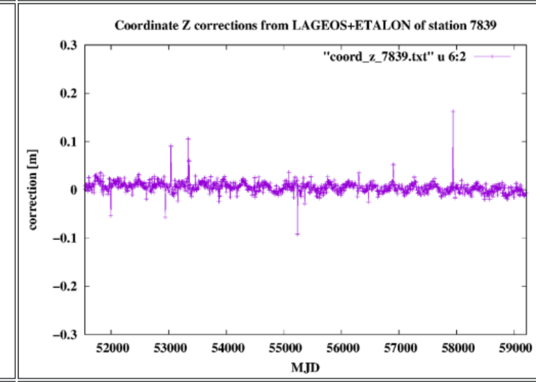
Herstmonceux 7840	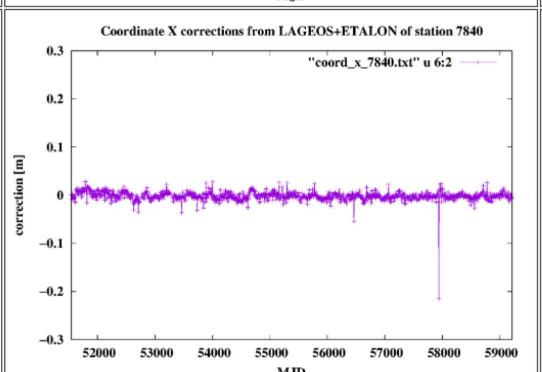	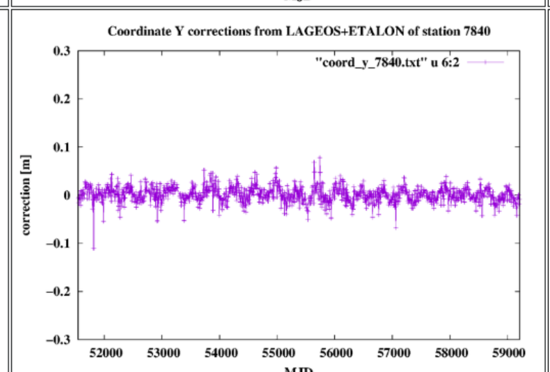	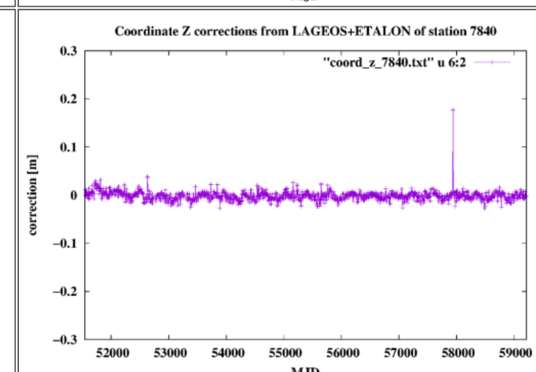

ITRF2020-Repro

SLR-derived Earth orientation parameters

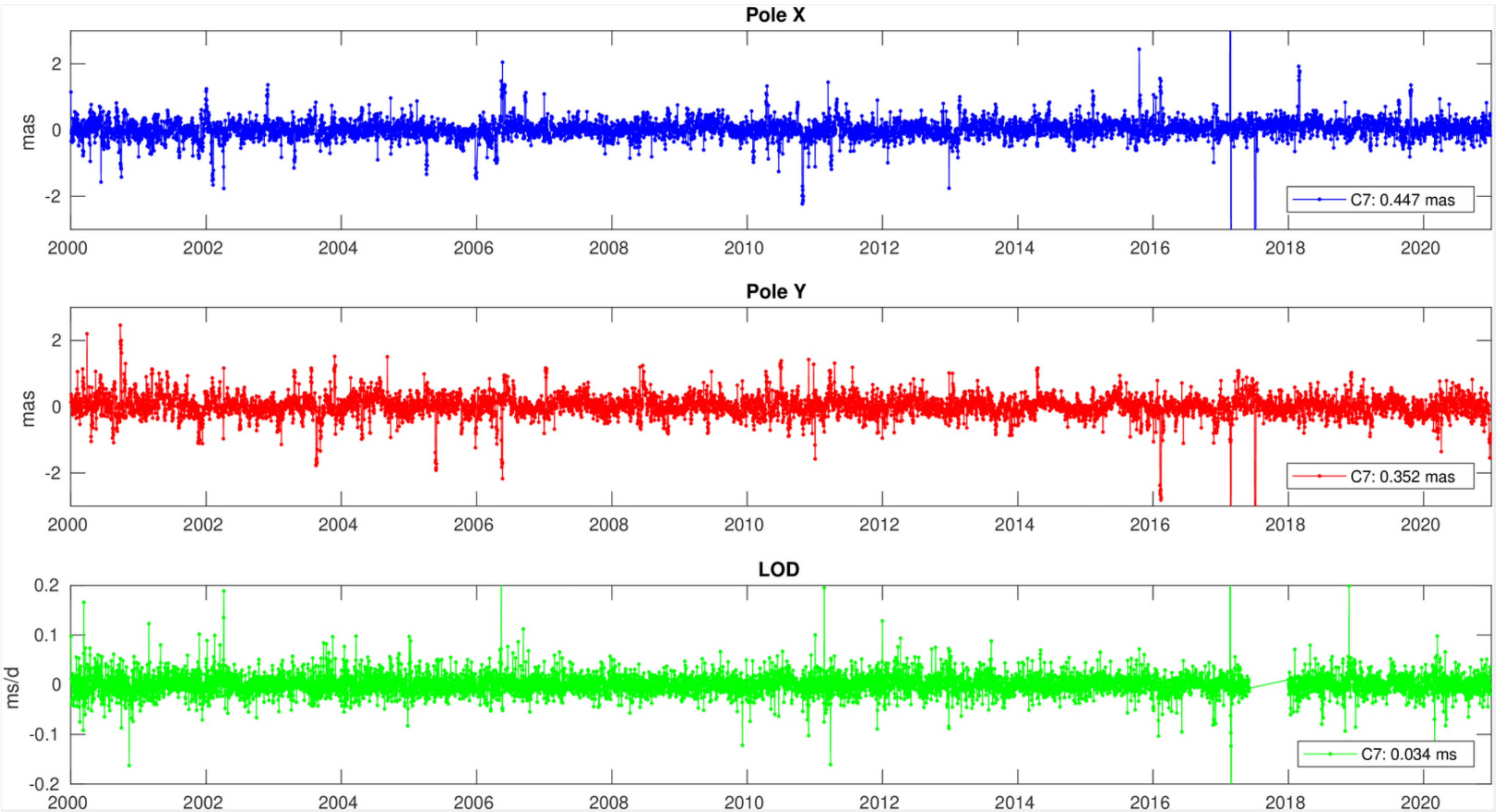

SRL Analyses of spherical satellites

Linda Geisser

Contribution of LARES to gravity field coefficients

- **Extension of the existing SLR processing at AIUB from the LAGEOS (A) and the ETALON (B) satellites to also include the low-orbiting satellite LARES (C)**

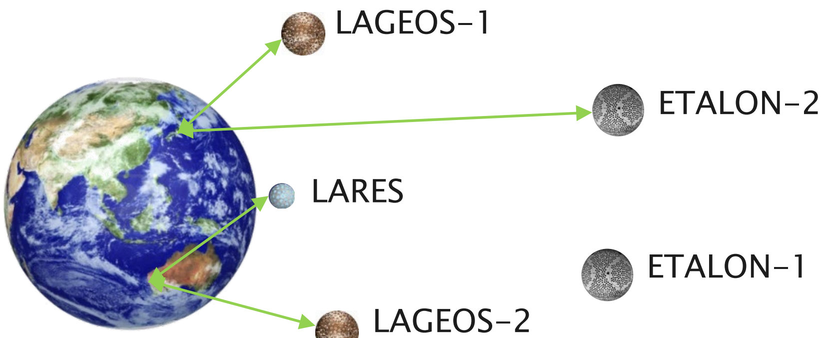

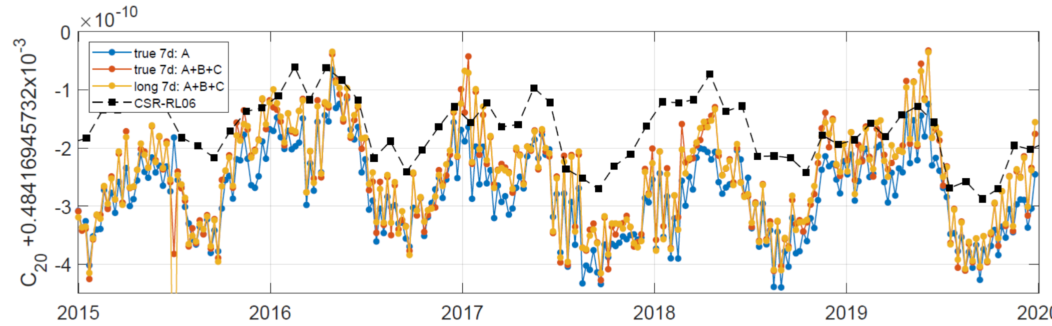

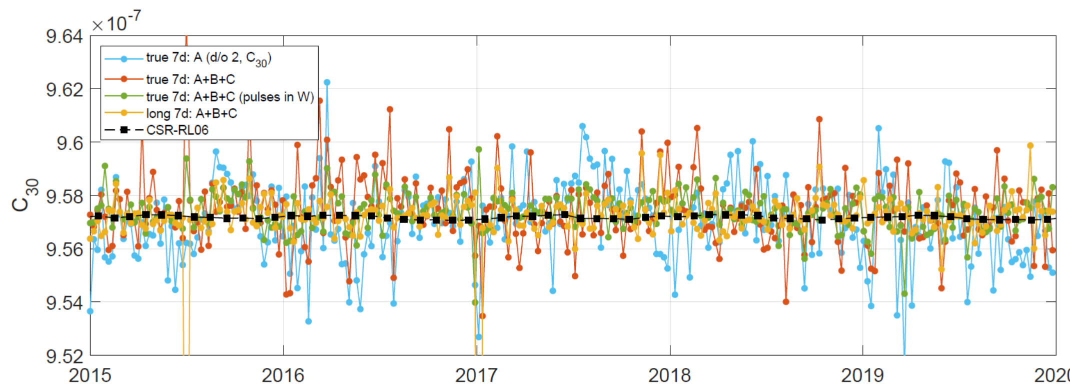

Homogeneous formation of SLR Normal Points

- **Different screening techniques of the SLR Fullrate data to build the SLR Normal Points**

RMS based rejection level (S1)

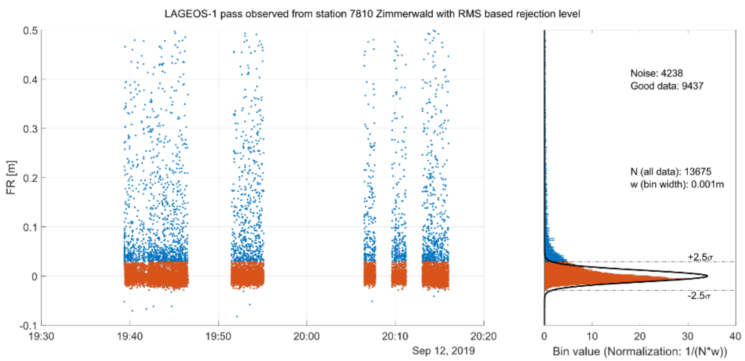

Leading edge method (S2) (Kirchner et al., 2008) (Wilkinson et al., 2018)

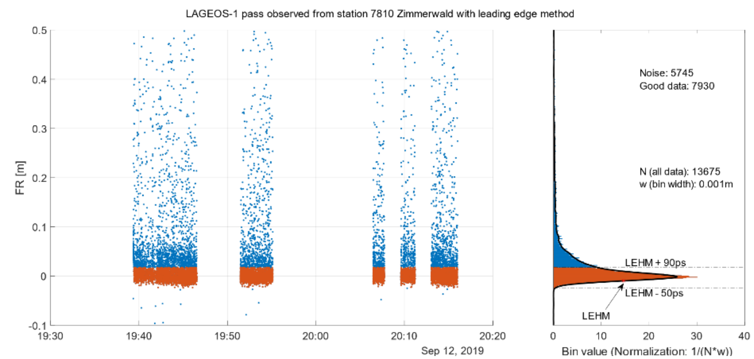

- **Differently derived SLR Normal Points have an impact on the estimated parameters in the SLR processing, e.g., on polar motion**

Sol	X pole $[\mu as]$		Y pole $[\mu as]$	
	Bias	WRMS	Bias	WRMS
S1	50,4	133,4	85,8	129,9
S2	48,4	128,9	97,1	126,7

Off-line analyses of LEO SLR data

Daniel Arnold

SLR Bias Determination Study

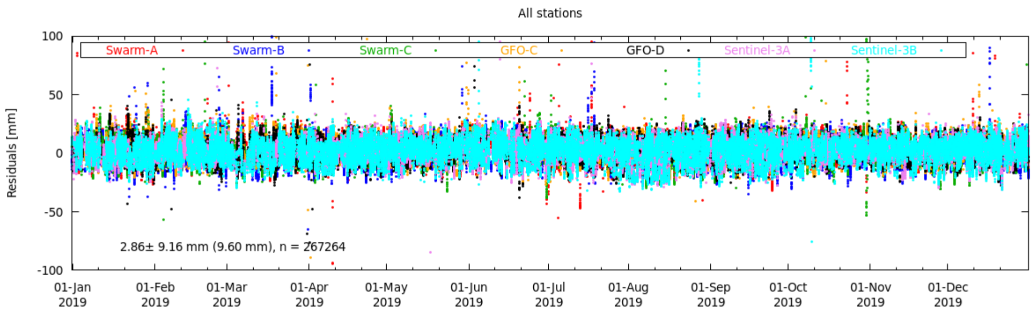

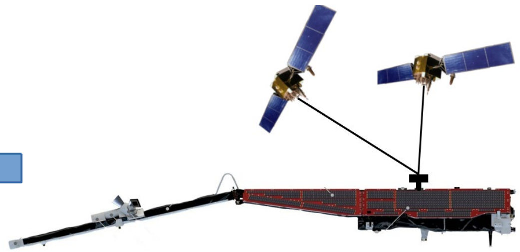

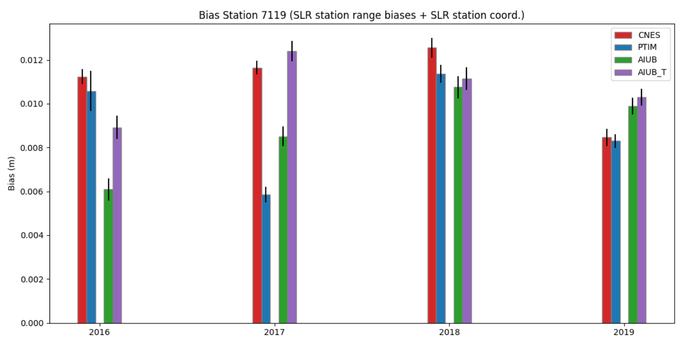

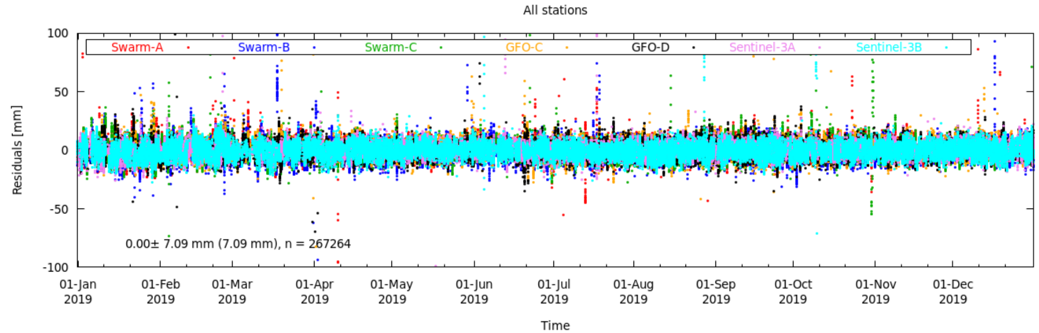

- Determine SLR station-related biases using independent multi-LEO GNSS- and DORIS-based orbits
- In the framework of the Copernicus POD QWG: AIUB, CNES/CLS, PosiTim, DLR

SLR Bias Determination Study

Clusters of SLR stations for which the range bias estimates of AIUB, CNES and PosiTim agree on different levels Δ (based on SLR data of 2019, when estimating range biases and coordinate corrections):

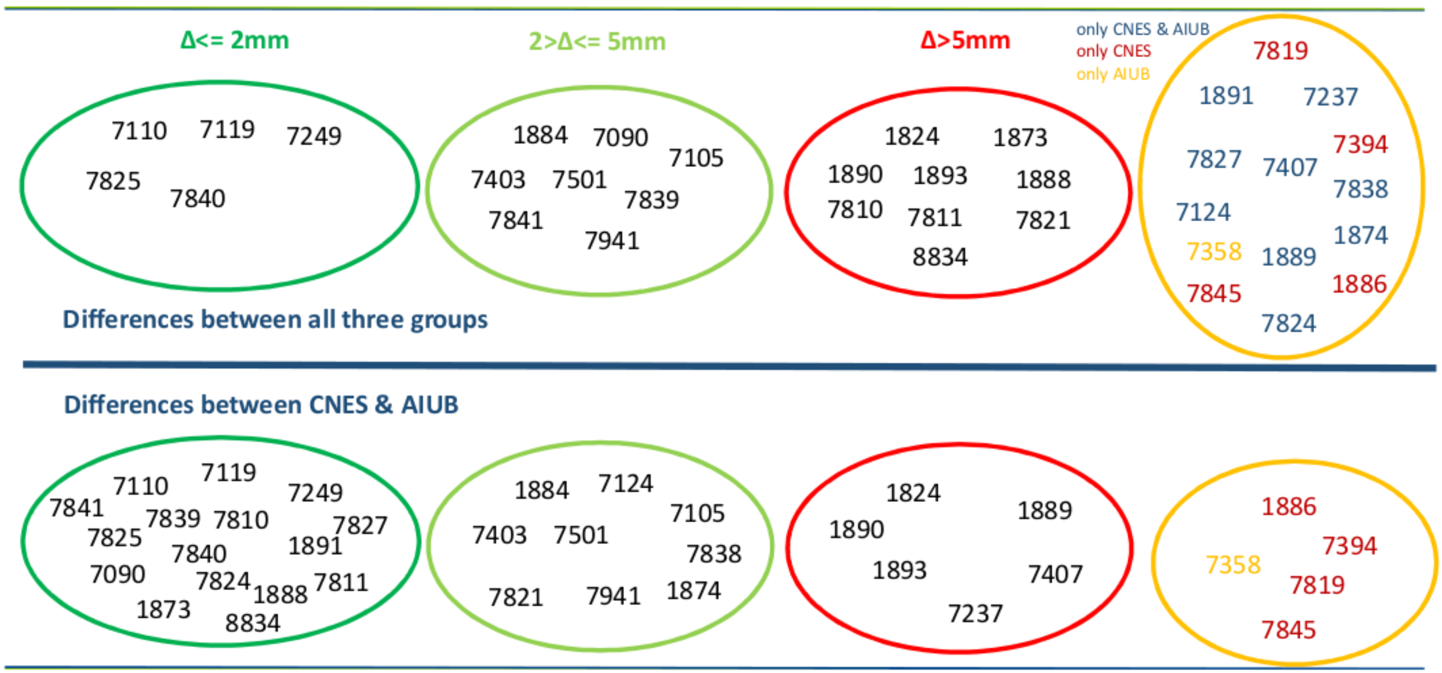

AIUB and CNES agree for 16 stations on range biases within 2mm, even when using independent orbits and softwares

Satellite Geodesy Research Group

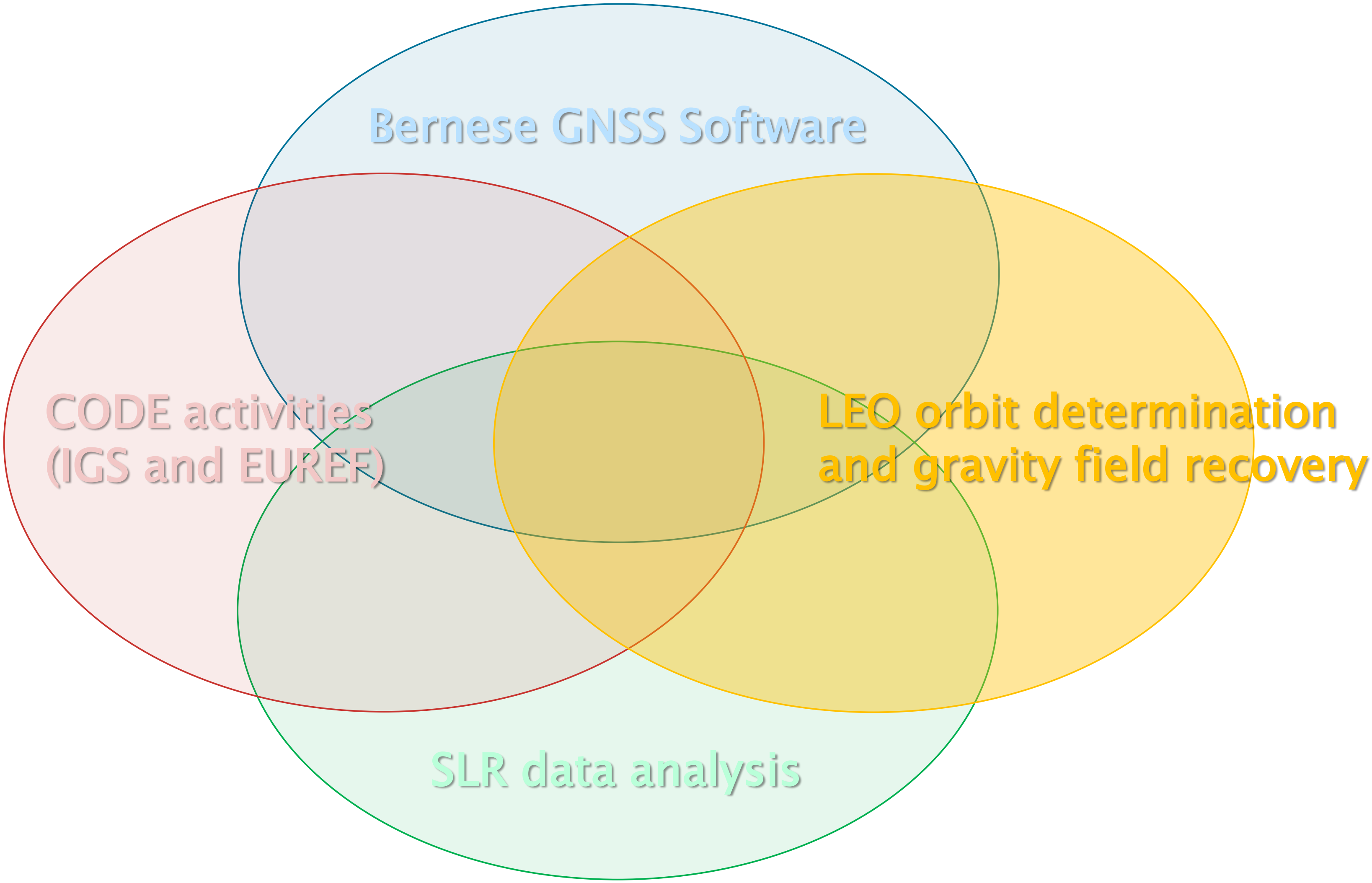

Copernicus POD Service

Daniel Arnold

Copernicus POD Service

At AIUB precise orbits of all Sentinel satellites are computed

Sentinel-1A
Sentinel-1B

Sentinel-2A
Sentinel-2B

Courtesy: ESA

Sentinel-3A
Sentinel-3B

Sentinel-6A

Copernicus POD Service

Two examples from Regular Service Review #21 (Apr-Jun 2021):

Differences of single Sentinel-3A solutions to a combined solution (AING: dynamic solution provided by AIUB):

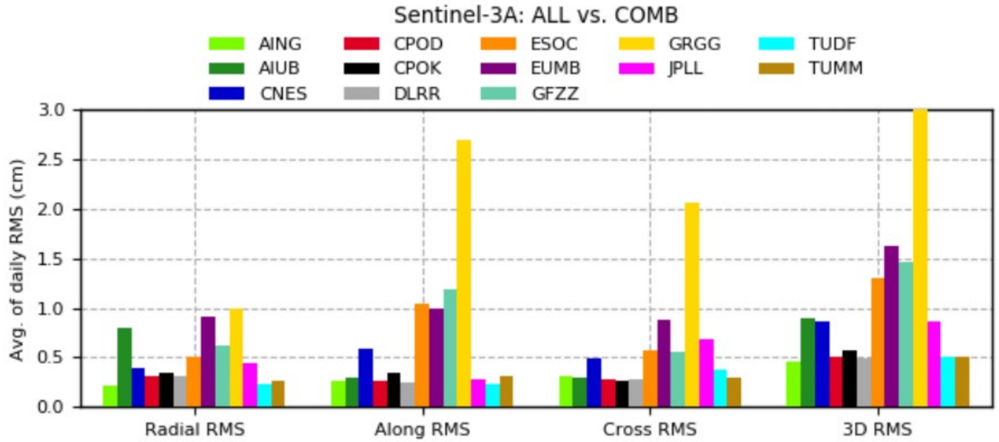

SLR residuals of Sentinel-6A AIUB orbits (biases fixed by GMV):

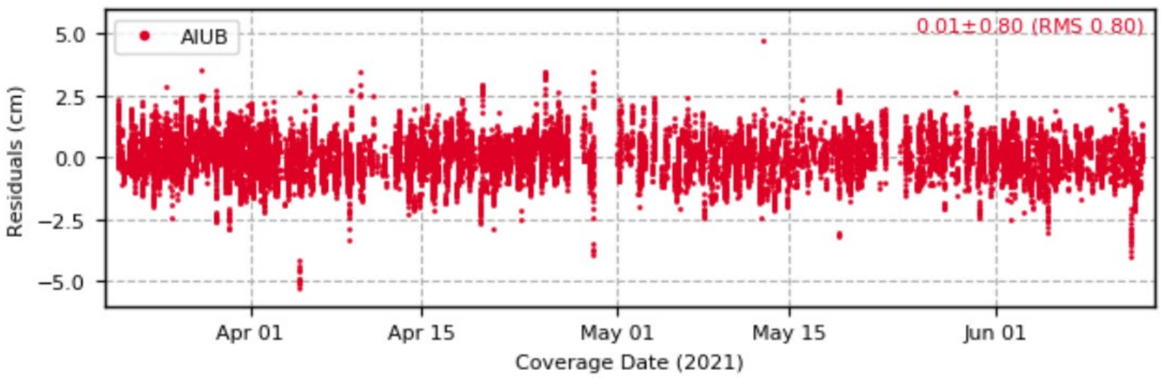

Copernicus POD Service

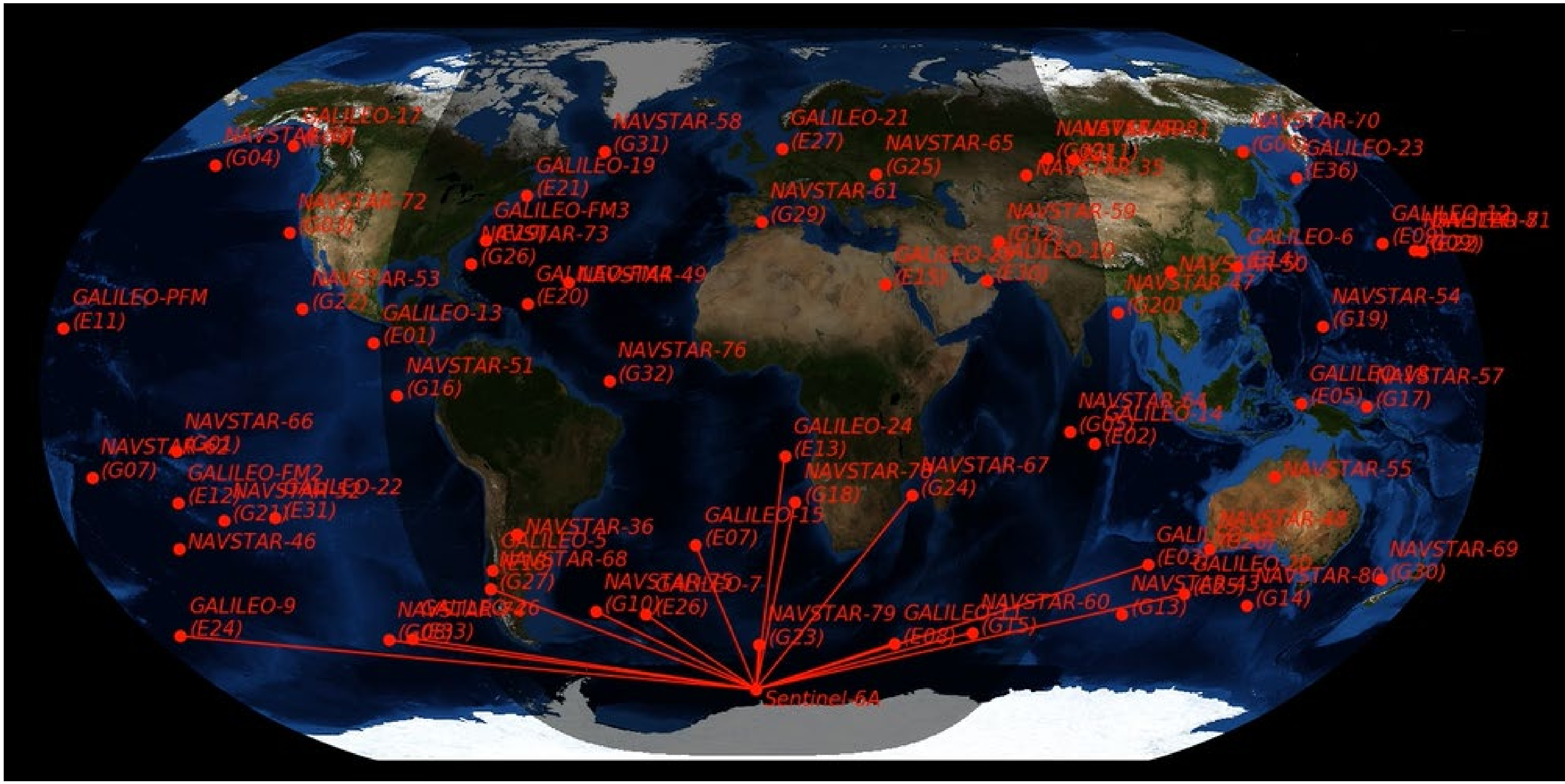

LEO POD Studies

Cyril Kobel

LEO Phase Center Offset estimation

Dynamic Precise Orbit Determination for all LEOs, Integer ambiguity fixing for all LEOs except Jason-2.

- Sentinel-1A/B
- Sentinel-2A/B
- Sentinel-3A/B

➢ Plausible results
➢ Constant values

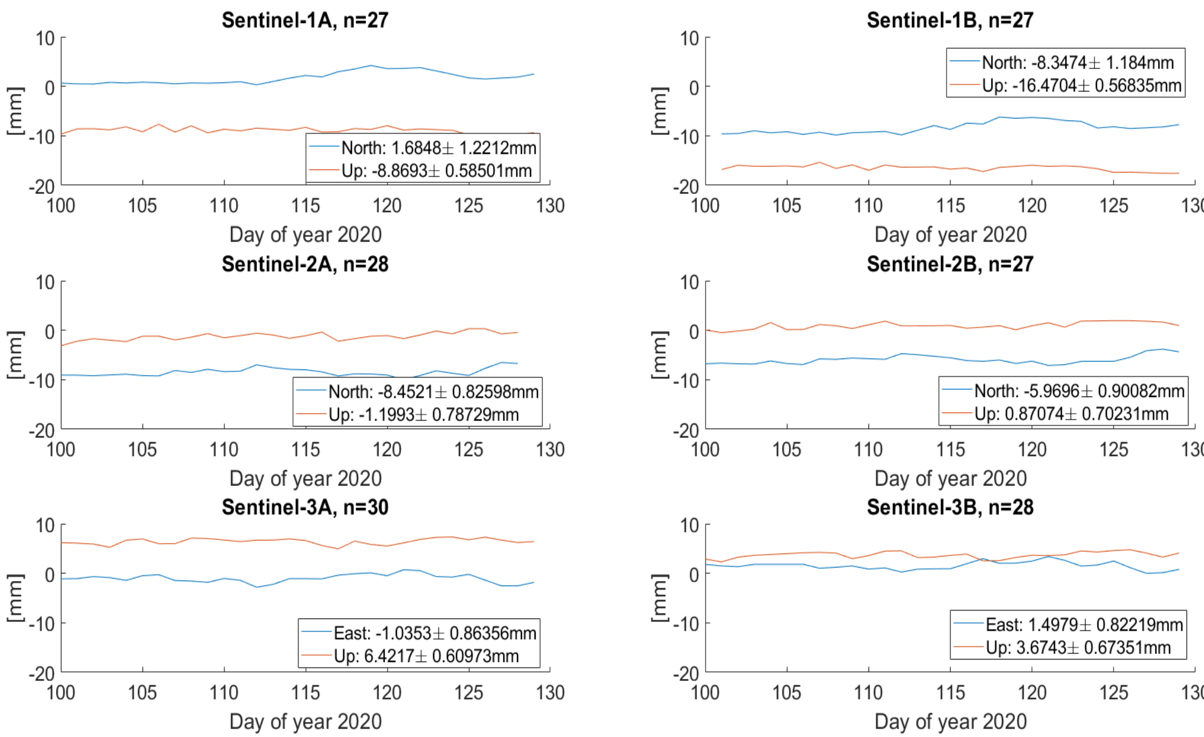

LEO Phase Center Offset estimation

Dynamic Precise Orbit Determination for all LEOs, Integer ambiguity fixing for all LEOs except Jason-2.

- Jason-2/3
- Perform yaw-steering/fixed-yaw attitude mode
- Estimated offsets in Up direction depend on attitude mode
- Yaw-steering: Estimation of North offset
- Fixed-yaw. Estimation of East offset

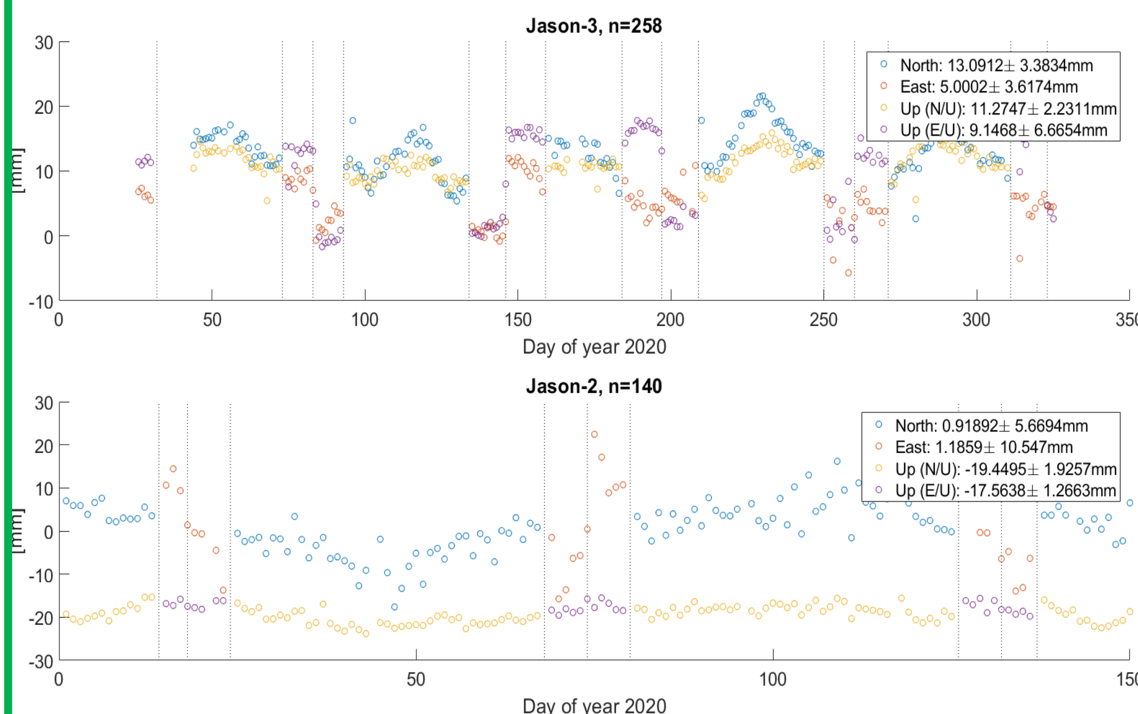

LEO topside ionosphere modeling

Lucas Schreiter

3D model formulation

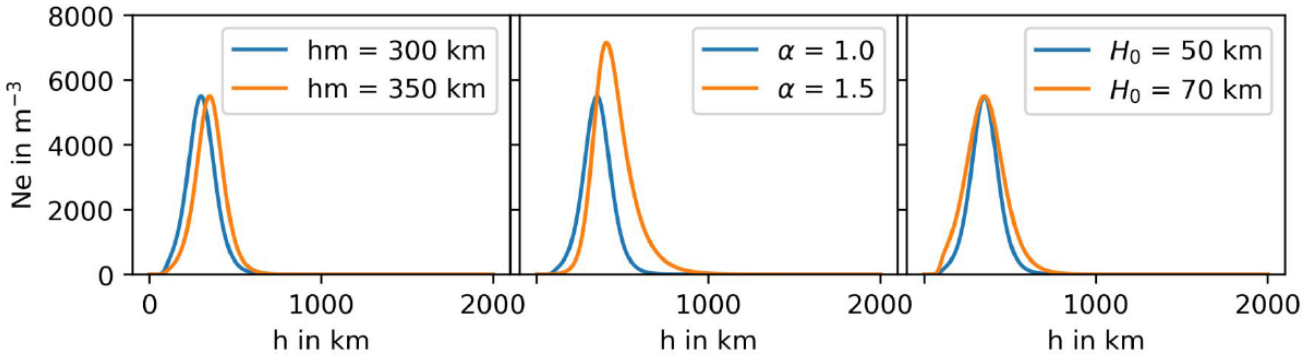

Epstein-Layer variation used as Profiler:

$$N_e(h) = 4N_m \frac{e^{\alpha z(h)}}{(1 + e^{z(h)})^2} \cdot \frac{e^{\bar{z}(h)}}{(1 + e^{\bar{z}(h)})}$$

Where $z(h) = \frac{h - hm}{H_0}$ and $\bar{z} = \frac{h - h_{cut}}{H_{cut}}$

N_m: Peak electron density
α: shape parameter
h: altitude
h_m: ionization peak altitude
h_{cut}: truncation altitude
H_0, H_{cut}: Scale height

$$Nm(mlat, mLT) = exp\left(\sum_{i=0}^{n_{Ne}} \sum_{j=-i}^{i} c_{Nm}^{(ij)} f_{ij}(mlat, mLT)\right)$$

$$hm(mlat, mLT) = f_{hm}\left(\sum_{i=0}^{n_{hm}} \sum_{j=-i}^{i} c_{hm}^{(ij)} f_{ij}(mlat, mLT)\right)$$

$$H_0(mlat, mLT) = f_{H_0}\left(\sum_{i=0}^{n_{H0}} \sum_{j=-i}^{i} c_{H_0}^{(ij)} f_{ij}(mlat, mLT)\right)$$

$$\alpha(mlat, mLT) = f_{\alpha}\left(\sum_{i=0}^{n_{\alpha}} \sum_{j=-i}^{i} c_{\alpha}^{(ij)} f_{ij}(mlat, mLT)\right)$$

- Spherical harmonics representation. f_* limits the values to valid ranges to avoid singularities
- Resolved up to degree and order 8

3h snapshots based on 11 LEO's

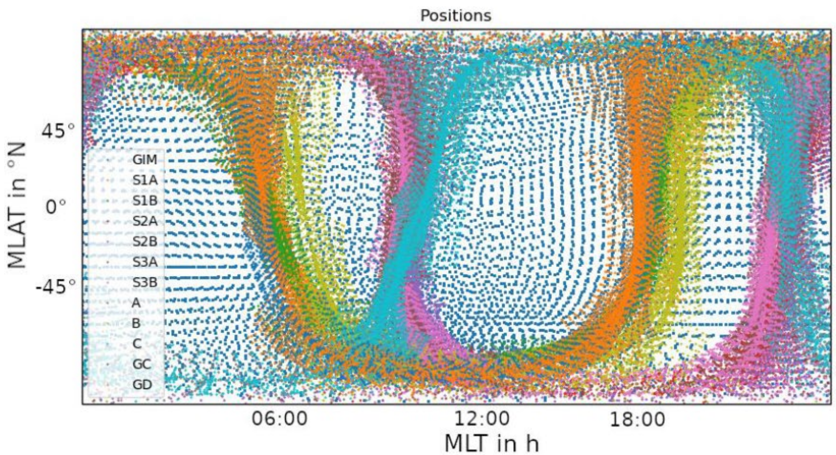

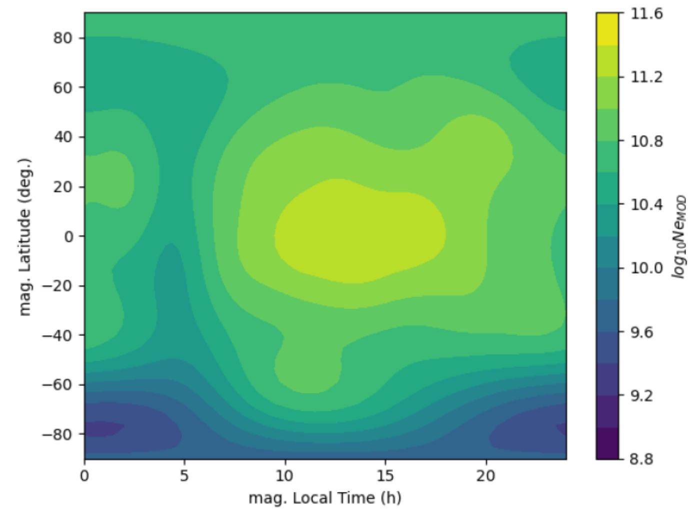

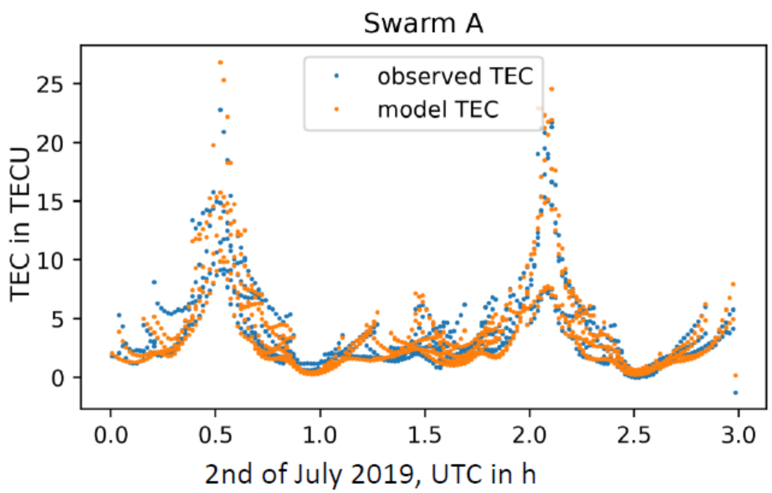

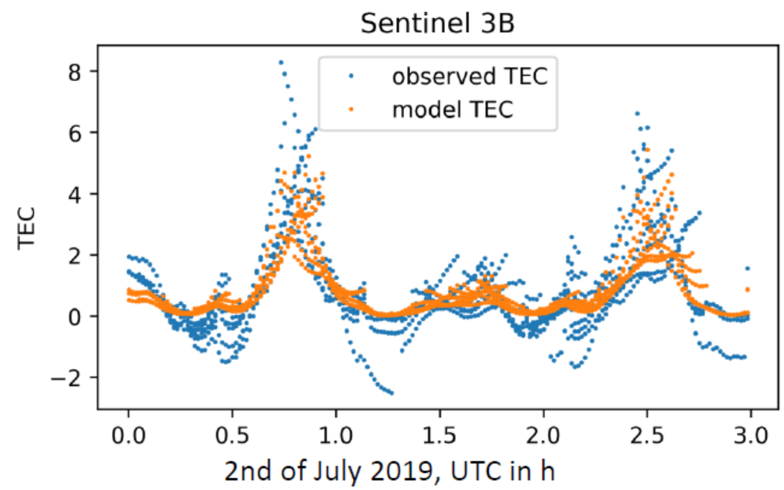

GRACE-FO Gravity Field Determination

Martin Lasser

Operational GRACE–FO processing

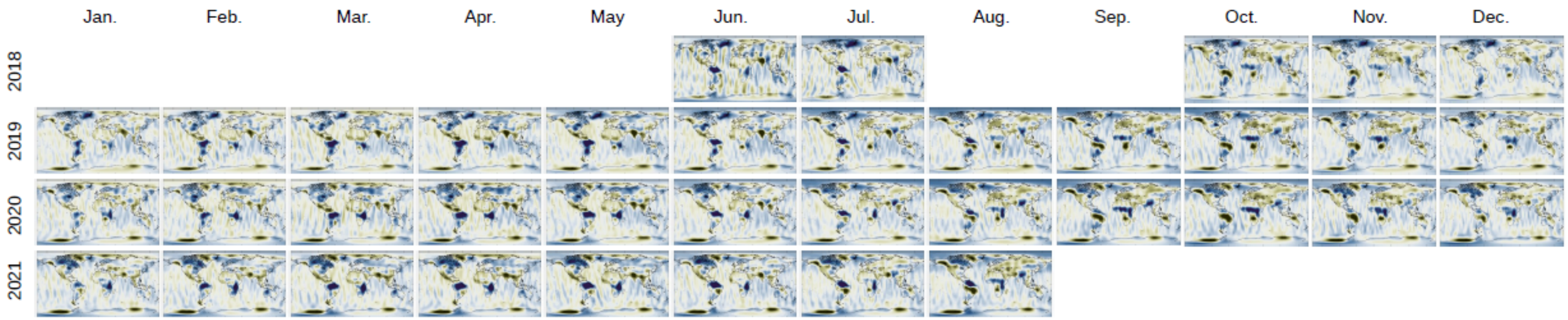

- operational since Sepember 2020
- available at ICGEM as AIUB-GRACE-FO_operational
- continuation of AIUB-RL02
- updated background models
- data screening with variance component estimation
- use of alternative GF2 Level 1B ACT product from IfG

Observation data screening for GRACE-FO

Observation data processing with VCE for 3 h blocks of normal equations

$$\left.\begin{aligned} r_k &= n_{obs} - \frac{\sigma_0^2}{\sigma_k^2}\,\mathrm{tr}\left(\mathbf{N}_k \mathbf{N}^{-1}\right) \\ \sigma_k^2 &= \frac{\boldsymbol{e}_k^T \mathbf{P}_k \boldsymbol{e}_k}{r_k} \end{aligned}\right\} \quad \hat{x} = \left(\sum_{k=1}^{n} \frac{\sigma_0^2}{\sigma_k^2} \mathbf{N}_k \right)^{-1} \sum_{k=1}^{n} \frac{\sigma_0^2}{\sigma_k^2} \boldsymbol{n}_k$$

Each block of observations gets a weight based on its contribution to the final solution

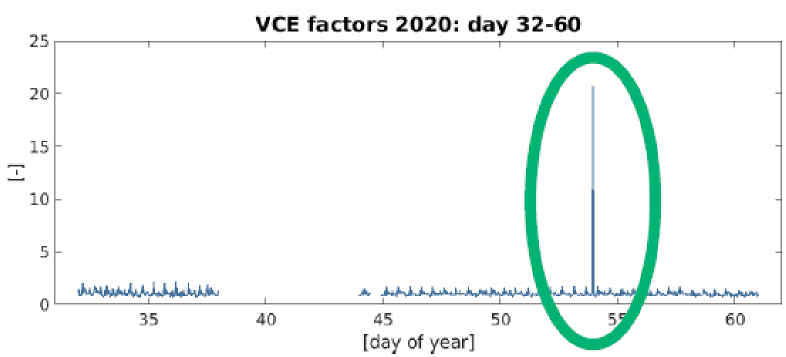

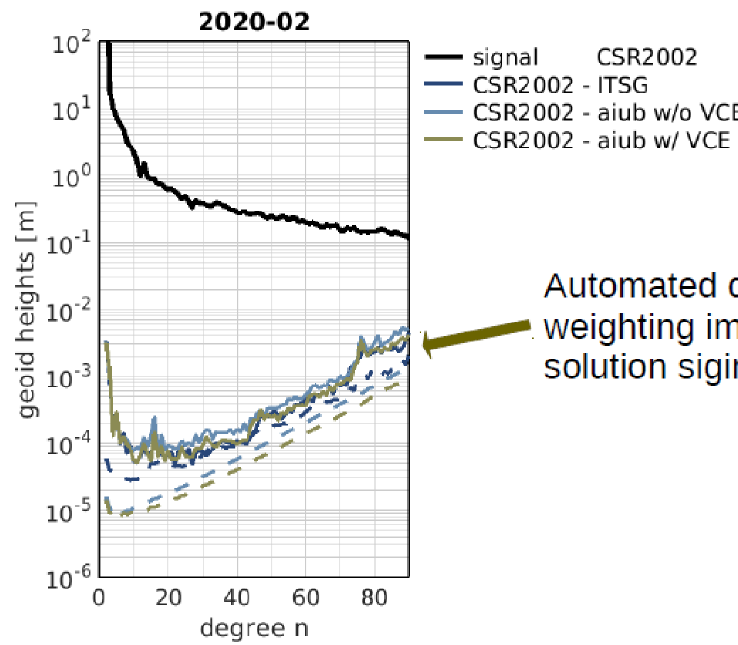

Automated data weighting improves solution siginficantly

Noise modeling for GRACE-FO

«op»

noise model:
- KBRR white noise 0.3 µm/s
- 15 min PCA per satellite in radial, along track, cross-track

«emp»

noise model:
- empirical covariances based on post-fit residuals

«theor»

noise model [Kim, 2000]:
- ACC coloured noise (red)
- KBR white noise

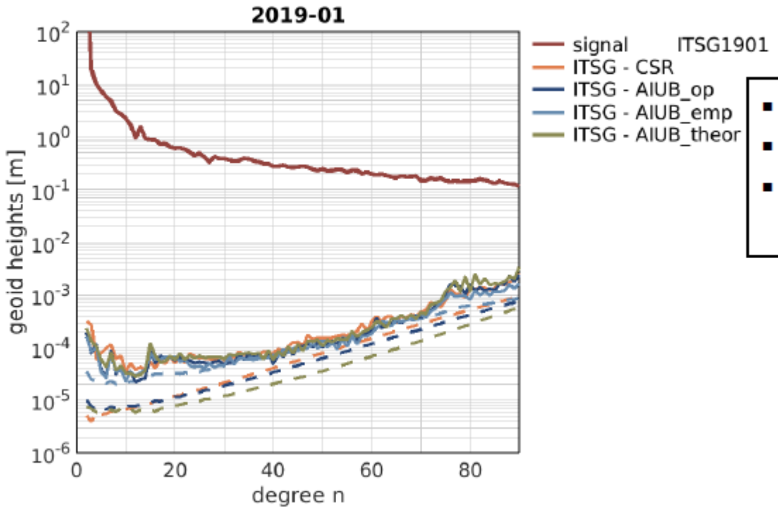

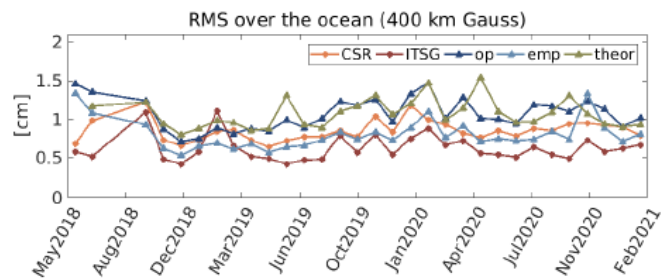

«op»
- flexible due to PCA
- absorbtion of deficiencies
- large number of (additional) paramters

«emp»
- formal errors → realistic
- no/few a priori knowledge
- iterations (costly on time)

«theor»
- a priori knowledge
- low RAM/CPU requirements
- might not reflect actual noise

Comparison KBR–LRI

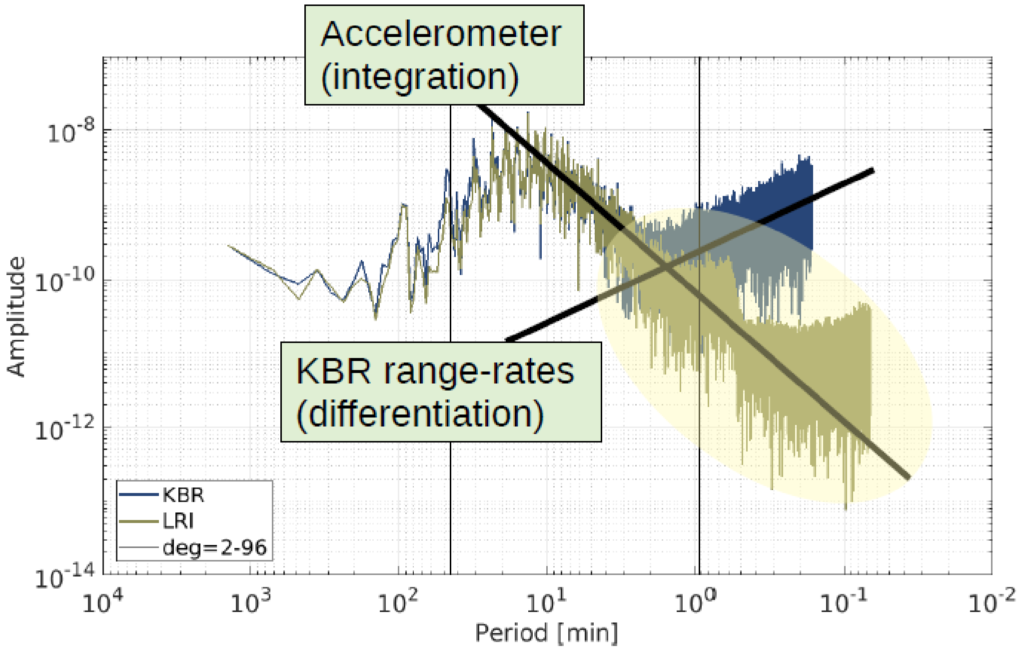

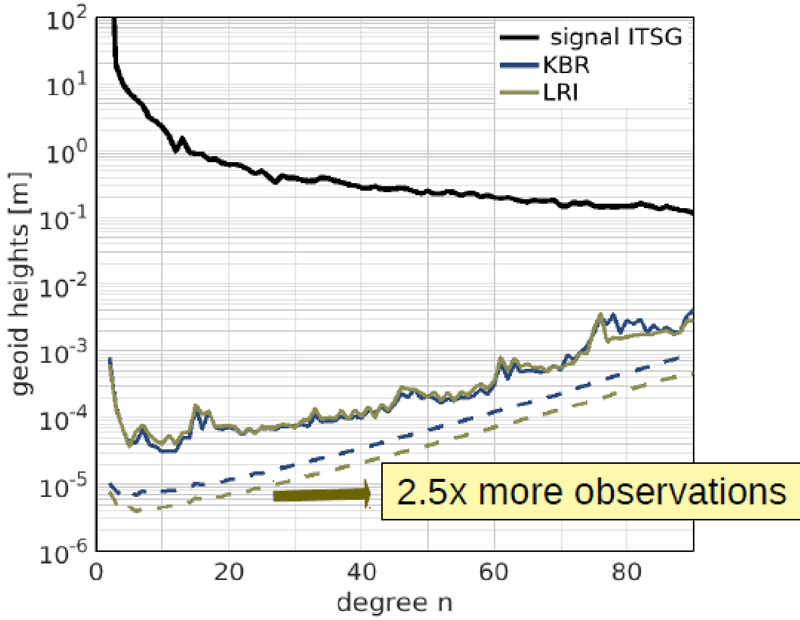

Amplitude spectrum of range-rate post-fit residuals
- clear improvement for LRI for periods < 3 min.

The reference is a K-band solution
- high LRI precision not visible

Combination Service for Time-variable Gravity Fields (COST-G)

Ulrich Meyer

GRACE-FO combination

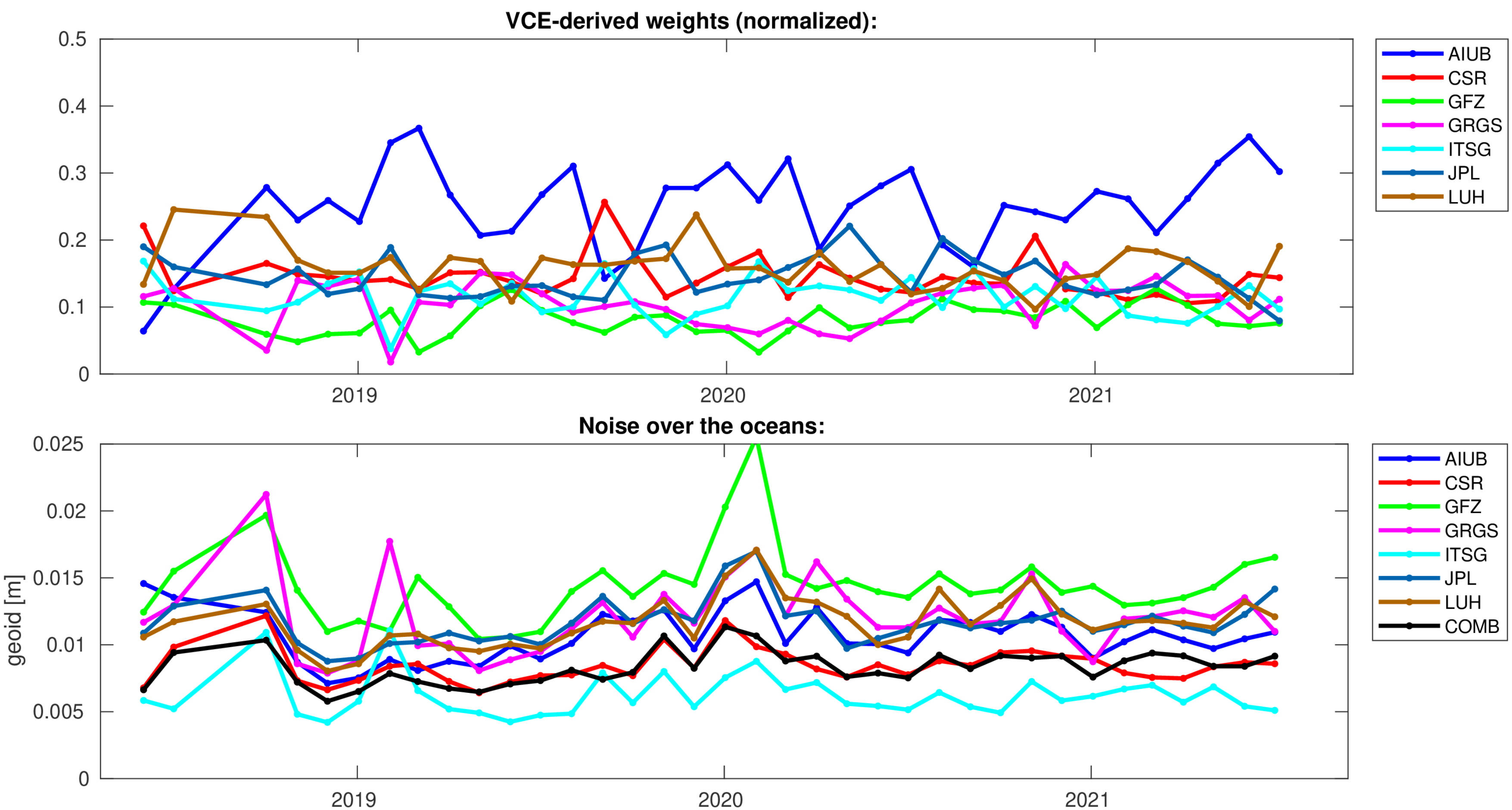

Since October 2021 the monthly GRACE-FO combination is performed with stable performance in operational mode.

Level-2 Products

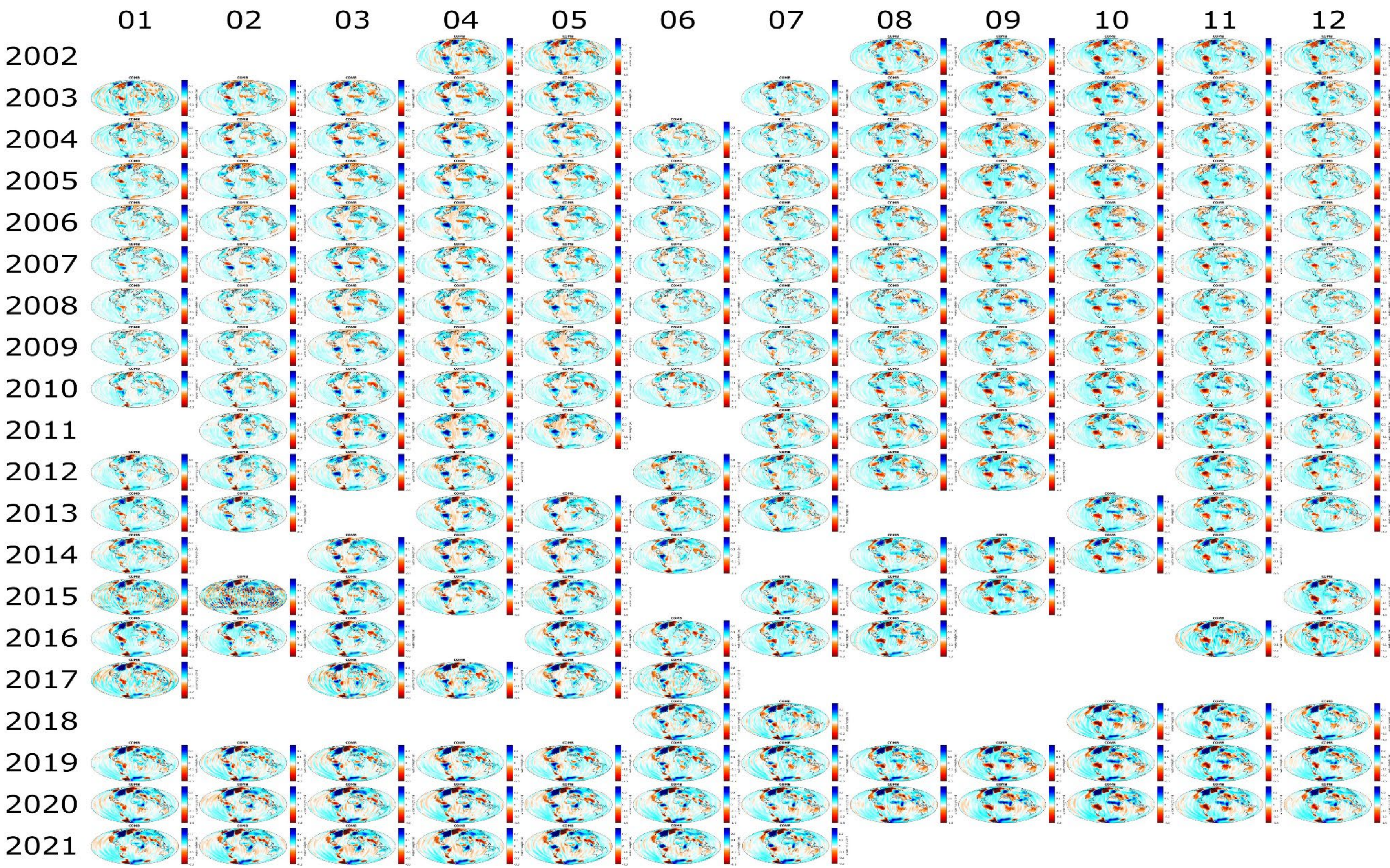

Gravity predictions for LEO-POD

COST-G

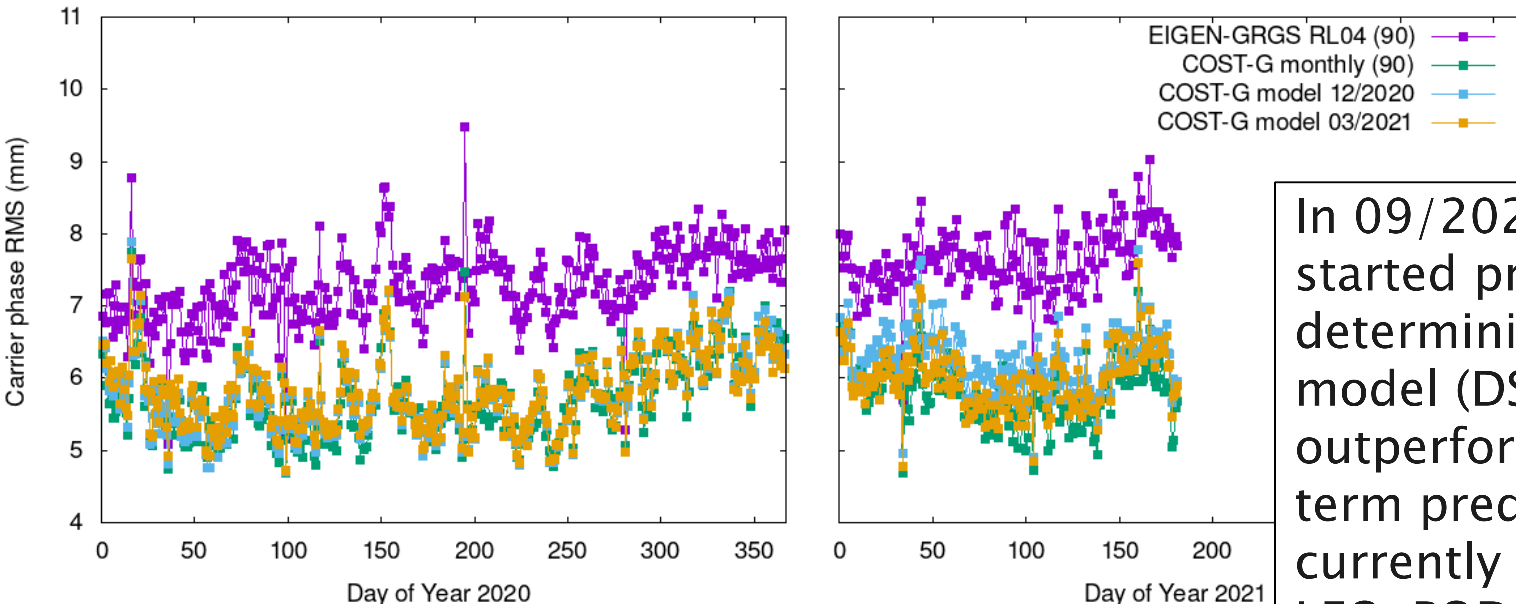

In 09/2021 COST-G started providing a deterministic signal model (DSM) that outperforms long-term predictions as currently used for LEO-POD.

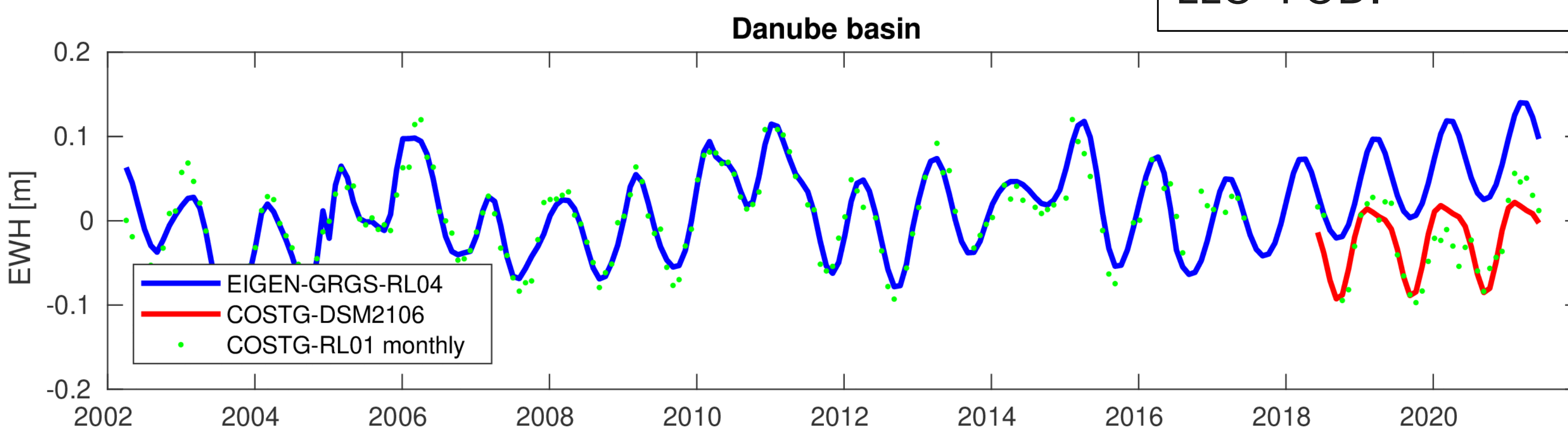

Gravity Field Determination from LEO GPS Data

Thomas Grombein

Gravity field time series based on LEO GPS data

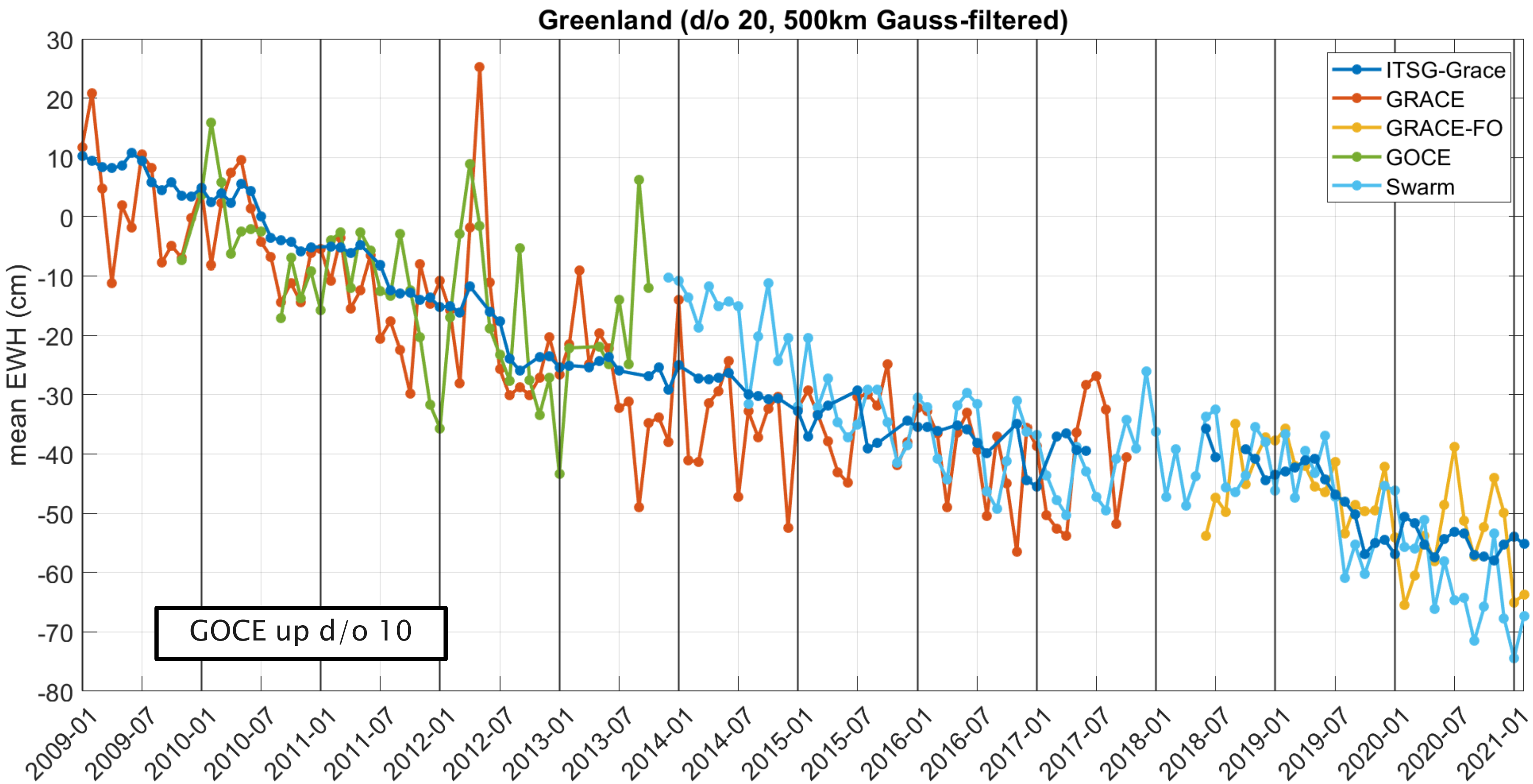

Gravity field time series based on LEO GPS data

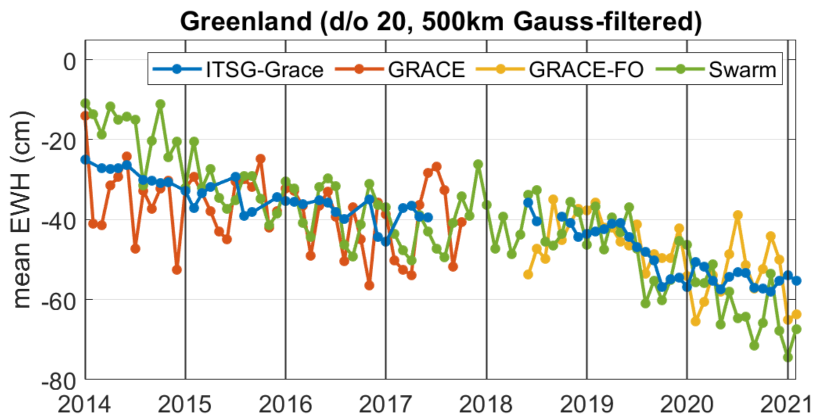

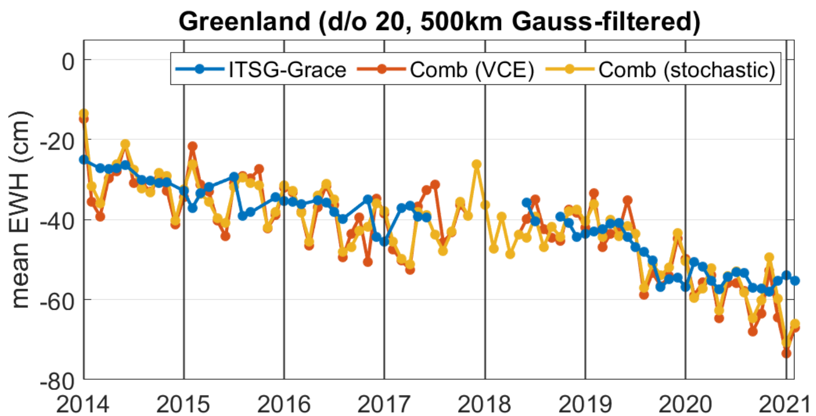

Nov
2016

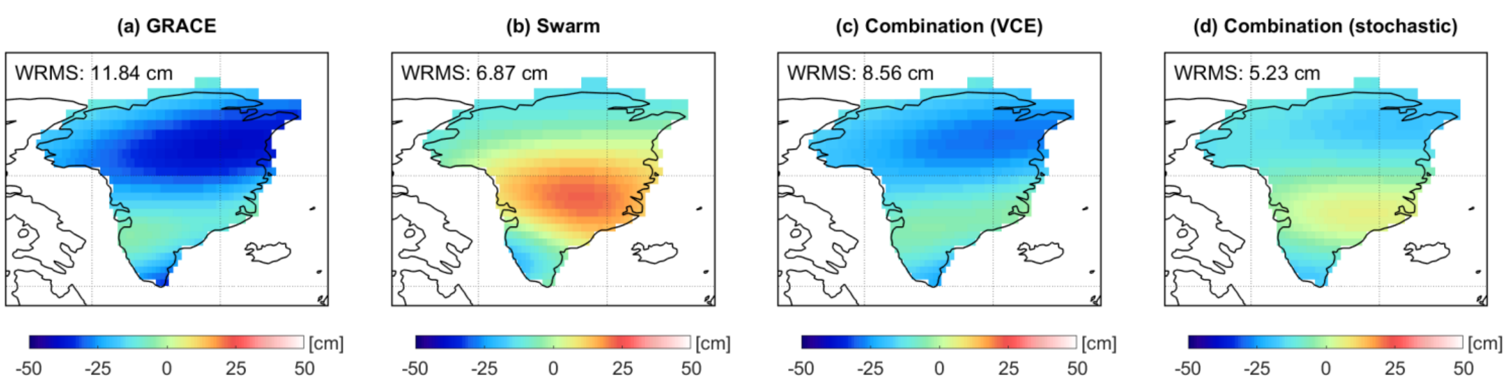

Simulation Studies in Planetary Geodesy

William Desprats

Orbit design and gravity field of Jovian moons

- Gravity field recovery using simulated Doppler observations from an orbiter around **Europa** and **Callisto**

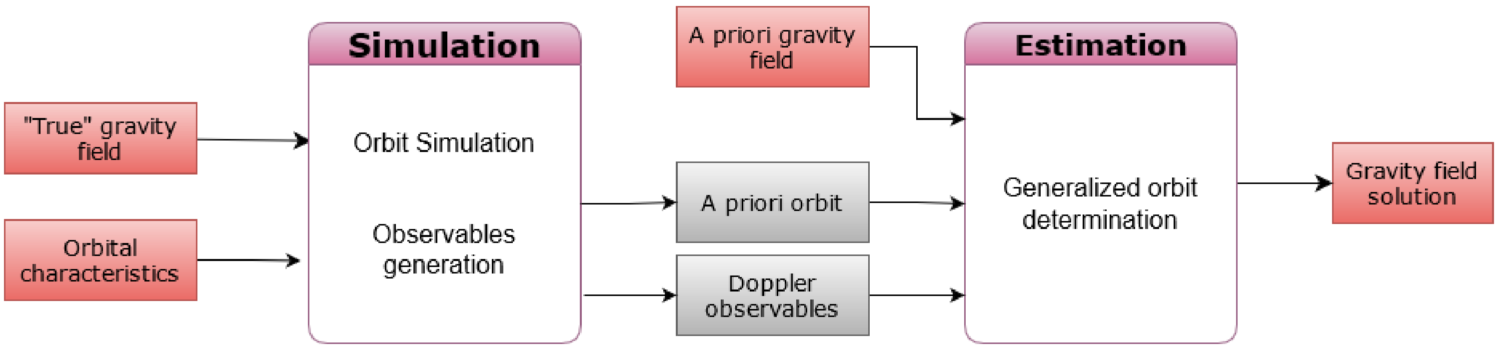

- Influence of key elements of orbit design were investigated separately:
  - Altitude
  - Inclination
  - Earth beta angle (see side plot for Europa)
  - Ground track repetition
  - Sun-Earth-Probe angle (plasma noise)

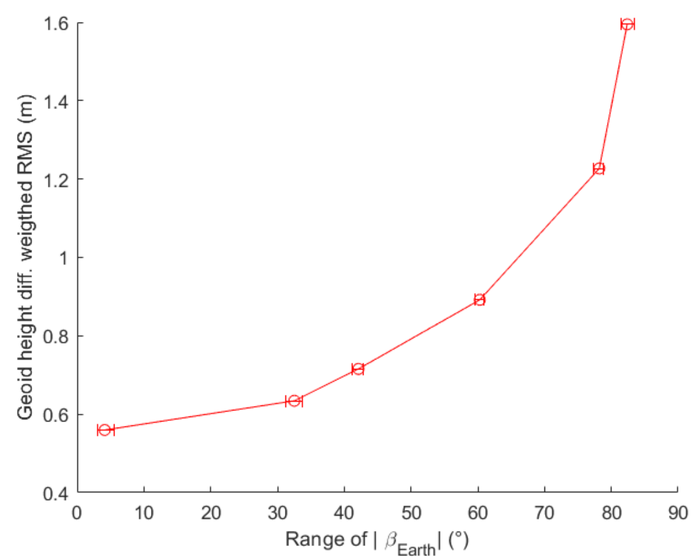

Non-Gravitational Accelerations around Callisto

- Different strategies to handle NGA (Solar and Planetary Radiation Pressure)
  - On-board accelerometer (10^{-8} m/s^2 white noise)
  - Pseudo-stochastic pulses (every 80mn = ½ orbital period)
  - 1 Cycle Per Revolution acceleration in radial and along-track directions

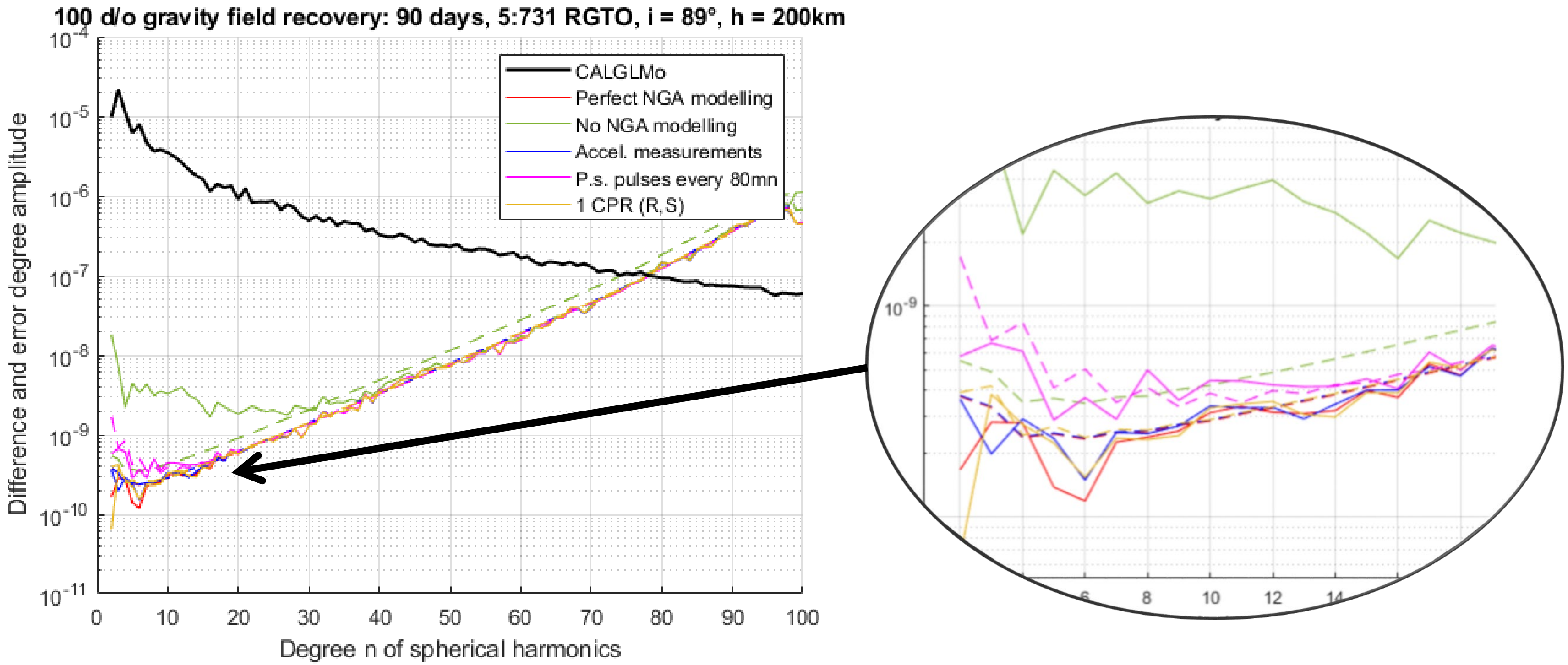

UNIVERSITÄT BERN

Swiss Optical Ground Station and Geodynamics Observatory Zimmerwald

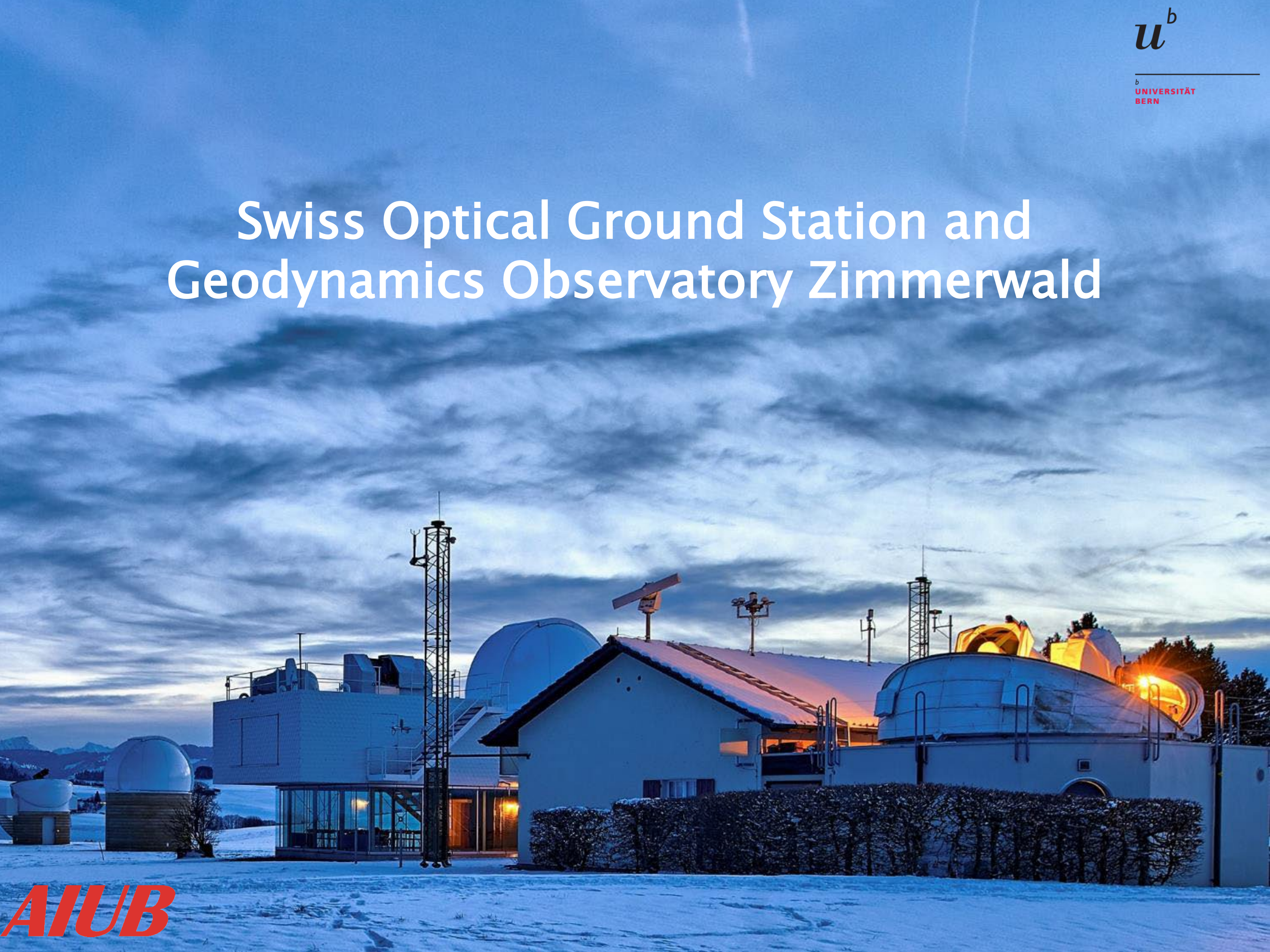

AIUB

Zimmerwald Team

M. Ackermann, P. Lauber, M. Prohaska, J. Rodriguez, T. Schildknecht, N. Zürcher

ZIML ILRS SLR Performance (last 12 Months)

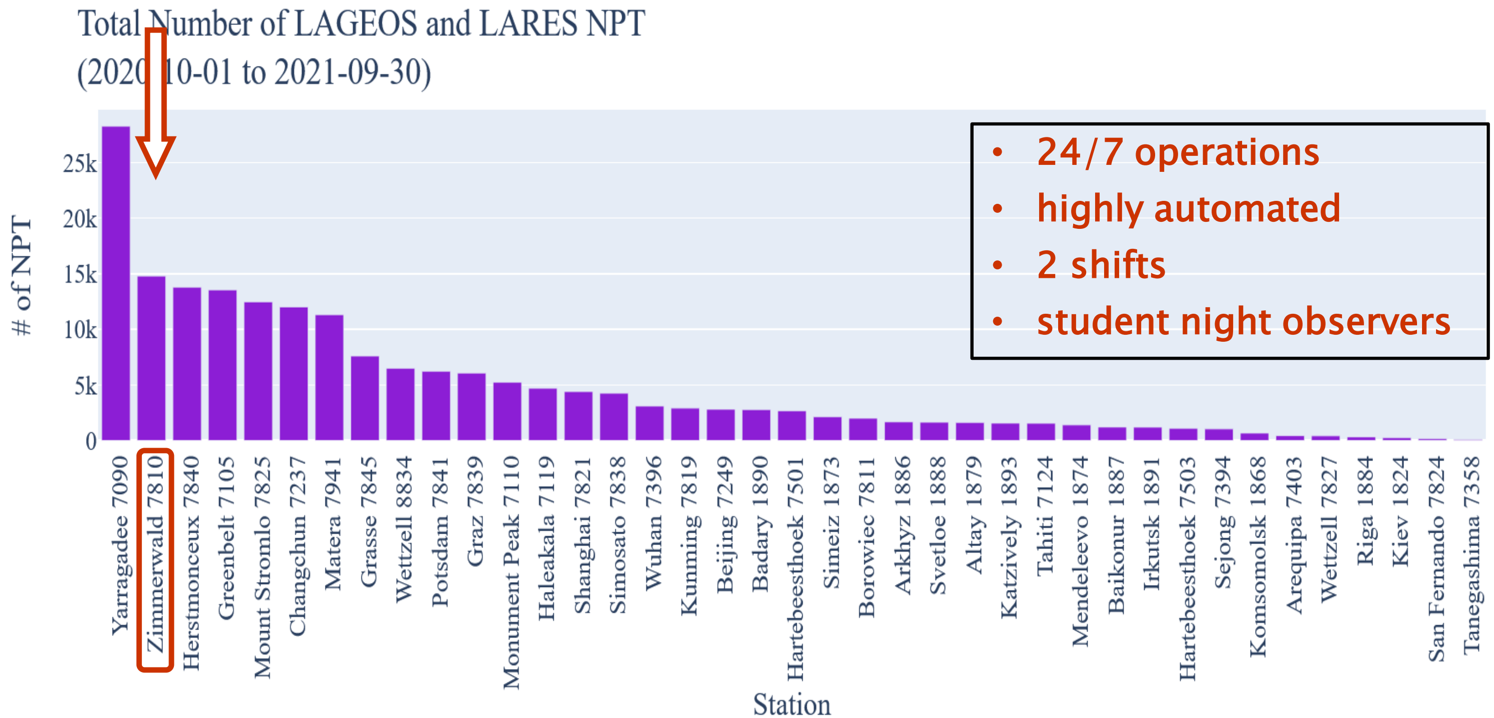

Best Week 2021

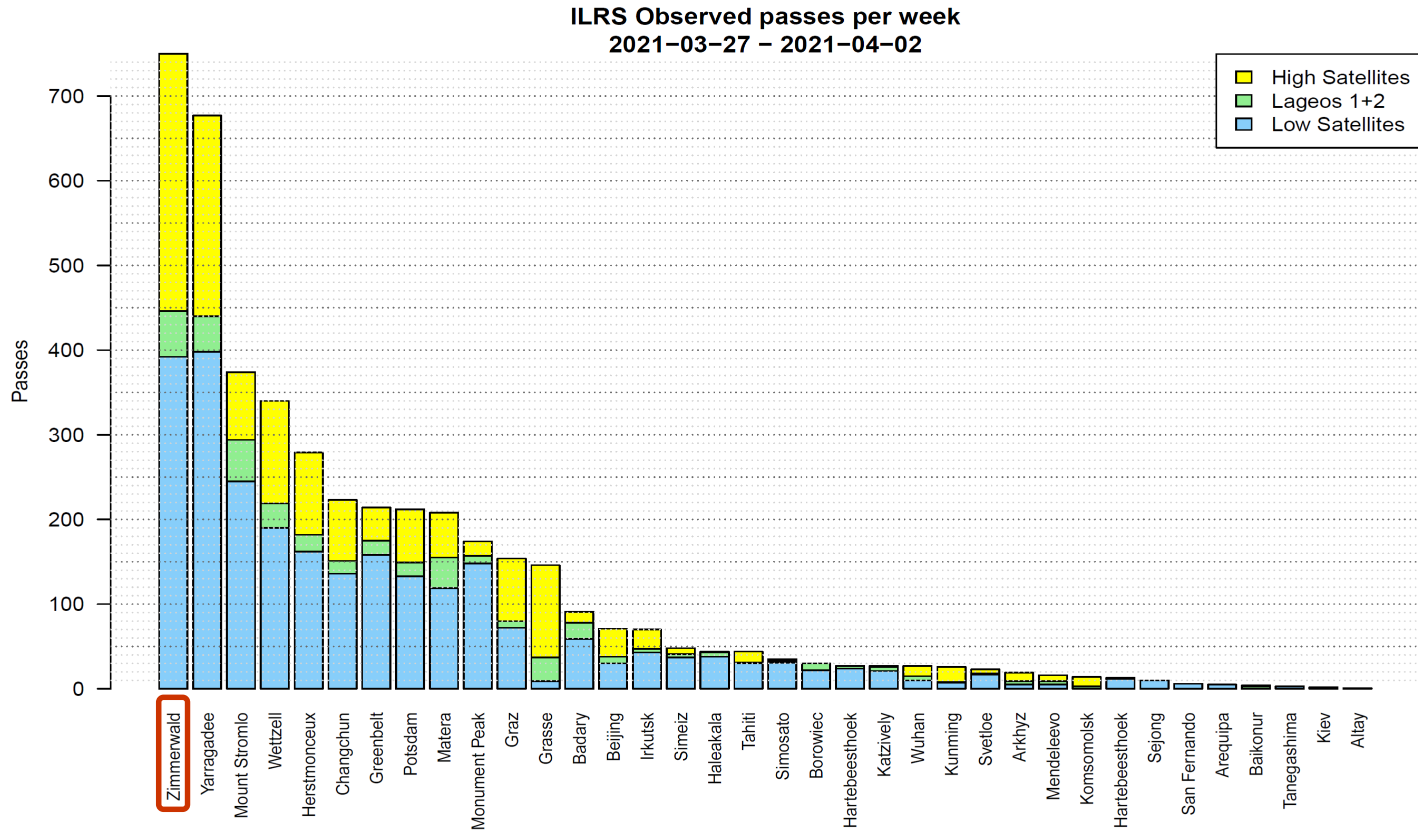

2nd Best Week 2021

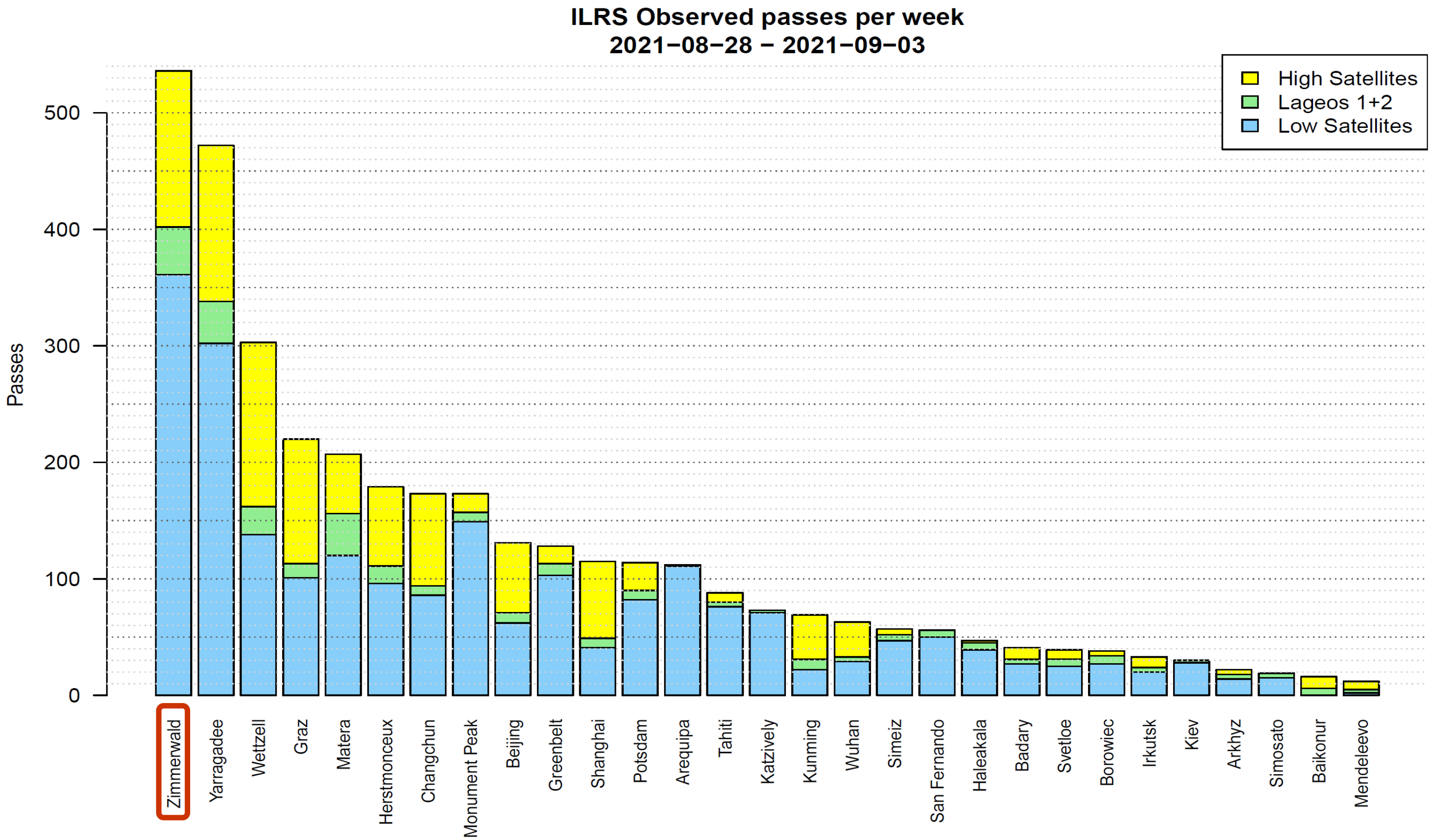

New 1kHz 10ps Laser System

- New 1kHz, 8 ps, 1.6 mJ @ 1064 nm!
- Acceptance test passed
- Will be mounted within a thermal box (actively cooled and heated for outdoor temperature compensation) on the ZIMLAT telescope tube (2022)
- Parallel operation with existing laser
- Goals:
  - increase accuracy from 12mm to 2mm
  - increase number of measurements by a factor of 10